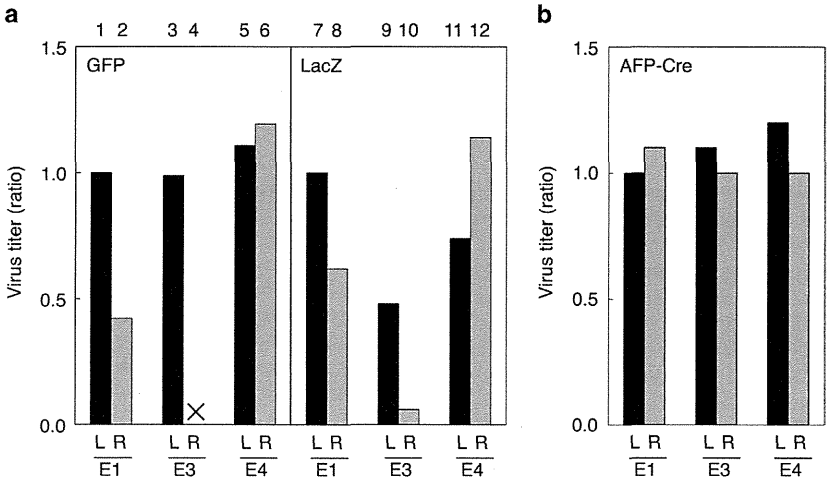

Figure 2. Titers of the virus vectors containing identical expression units. (**a**) Virus titers of the AdVs containing the EF1α promoter. The AdV genomes transduced into the HuH-7 cells were measured 3 days post infection. The virus titers were calculated relative to the copy numbers of the AdVs.[16] The titer of the E1L vector was set as 1; G-E1L, 8.3×10^8 relative virus titer (rVT)/ml, L-E1L, 5.0×10^9 rVT/ml. '×' indicates that G-E3R could not be obtained. (**b**) The titers of the virus vector containing Cre gene driven by the AFP promoter. E1L vector was used as the control. $^*P < 0.05$, $^{**}P < 0.01$.

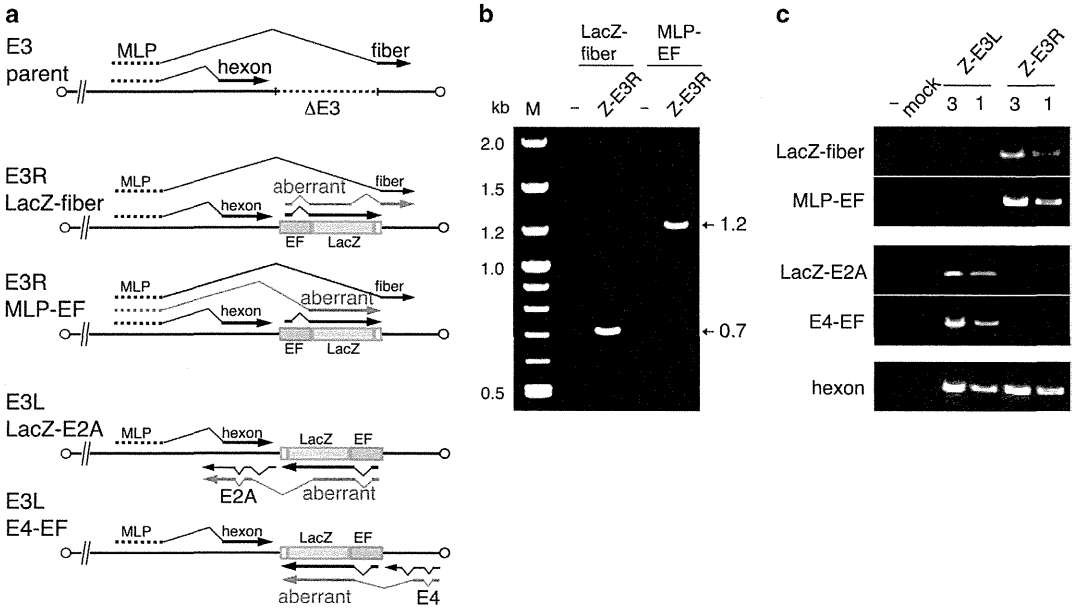

Figure 3. Structures of aberrant chimeric mRNAs. (**a**) Schematic representation of the aberrantly spliced mRNA and the expression unit in the E3 region. The LacZ expression units in the E3 region are shown. Aberrant mRNAs are shown in red. The bold lines and thin polygonal lines represent the exon and intron of the transcript, respectively. Arrow, orientation of the transcription; EF, EF1α promoter; LacZ, LacZ DNA. The 'parent' denotes the vectors before the insertion into the E3. 'LacZ-fiber,' 'MLP-EF,' 'LacZ-E2A' and 'E4-EF' indicate combinations of primers for detection of the chimeric mRNAs. (**b**) Detection of aberrant splicing by PCR. The 293 cells were infected with the Z-E3L and Z-E3R vectors, as indicated. The bands are generated from the chimera-specific mRNA between the viral gene and the inserted transgene. The primer sequences are shown in Supplementary Table S2. M, size maker; -, no DNA. (**c**) Specificity of the aberrant splicing. The 293 cells were infected with either Z-E3L or Z-E3R. The splicing from the MLP to hexon was used as the control. The bands of LacZ-fiber and MLP-EF in Z-E3R are the same as those described in (**b**) (0.7 and 1.2 kb, respectively). These bands were not detected in Z-E3L (lanes 3 and 1); threefold more DNA was loaded in lane 3 than in lane 1 to clearly show the semi-quantitative difference in the amount of cDNA. mock, mock infection of the 293 cells.

from the MLP donor to the EF1α acceptor and from LacZ donor to the fiber acceptor. We confirmed that these LacZ-fiber and MLP-EF aberrant mRNAs observed for the Z-E3R vector were not detected for the Z-E3L (Figure 3c, first and second rows).

We further examined whether such abnormal chimera mRNA was present for the Z-E3L vector of the opposite orientation. Actually, we detected two chimera mRNAs using the same PCR analysis; a viral E4 donor was spliced to the EF1α acceptor, and the

cryptic LacZ donor was spliced to a viral E2A acceptor (Figure 3a, fourth and fifth; Figure 3c, third and fourth rows. They were not detected for Z-E3R). The EF1α acceptor and LacZ donor were the same as those found in the E3L vector, and the sequences of the viral donor and the acceptor were identical to those found in the wild-type adenovirus, although the combinations were abnormal (Supplementary Table S1).

Then, we measured the amounts of fiber mRNA for the Z-E3R vector (very low titer) and compared them with those for the Z-E1L vector (high titer) and Z-E3L vector (medium titer) by conventional PCR and quantitative PCR (qPCR). These PCR and qPCR primers were designed to detect specifically the normal MLP-fiber mRNA, but not the aberrant mRNA, because they are prepared at the sequence junction: the forward and reverse primers are located in the MLP and fiber, respectively. The cDNAs from the 293 cells infected with Z-E1L, Z-E3L or Z-E3R were diluted from 10^0 to 10^{-3} before PCR (shown as '0' to '−3' in Figure 4a) for semi-quantitative detection (Figure 4a). The level of normal fiber mRNA of Z-E3L (middle titer) was lower and that of Z-E3R (very low titer) was much lower than that of Z-E1L (high titer), that is, the fiber mRNA levels and titers were well correlated. Notably, the amount of fiber mRNA of the Z-E3R vector was only 2% of that for the Z-E1L vector (Figure 4b, E3R). This may probably explain why the titer of Z-E3R was very low.

The expression of the E1 transgenes was higher than that of the E3 or E4 transgenes

The titers show amounts of infections virus particles produced by the vectors growing in the 293 cells, while expression levels are also important for the vector. The amounts of the produced gene products being influenced by the position of an identical expression unit on the cell chromosomes is referred to as the 'position effect' of gene expression.[13,14] To examine whether identical transgenes inserted into vector genomes are influenced or not by the 'position effect,' we infected the HuH-7 cells with the same numbers of active vector particles[16] expressing GFP under the control of the EF1α promoter at multiplicity of infection (MOI) 3 and 10 and measured the amounts of GFP mRNAs by qPCR (Figure 5a).

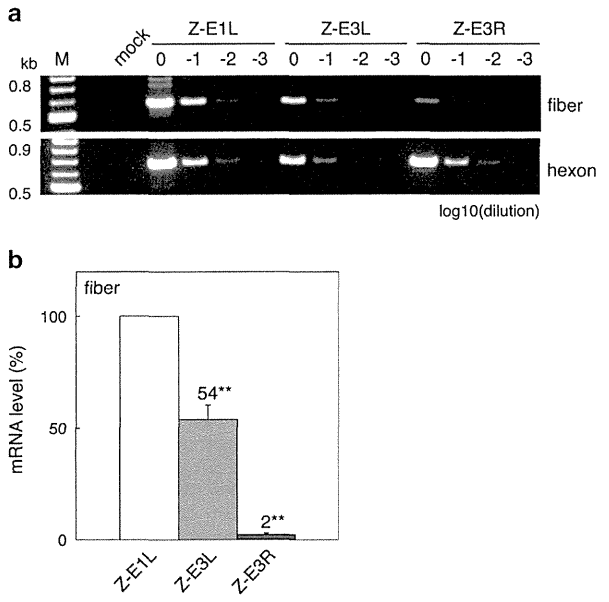

Figure 4. The relative levels of fiber mRNAs. The 293 cells were infected with the Z-E1L, Z-E3L and Z-E3R at MOI 5. (**a**) PCR detection of the fiber and hexon mRNAs. '0, -1, -2 and -3' mean '10^0, 10^{-1}, 10^{-2} and 10^{-3} dilution of the cDNAs', respectively. M, size marker; mock, mock infection of 293 cells. (**b**) The quantities of the fiber and hexon mRNAs determined by qPCR. Amount of fiber mRNA relative to those of each hexon and Z-E1L fiber are regarded as 100%. $n=3$; means ± s.d. ** $P<0.01$.

E1L and E1R vectors expressed much more GFP mRNA than the other three vectors, that is, the E3L, E4L and E4R vectors, both at MOI 3 and MOI 10 (bars 2 and 3 to 4, 6 and 7; bars 8 and 9 to 10, 12 and 13). In regard to the expression levels of these vectors, the mRNA amounts of the E4 vectors were about one-third of those of the E1 vectors. Similar results were obtained for the vectors expressing LacZ: E1L/R vectors expressed much more LacZ mRNA than all the E3 and E4 vectors, both at MOI 3 and MOI 10 (Figure 5b, bars 2 and 3 to 4–7; bars 8 and 9 to 10–13). Therefore, similar effects were observed using two different genes. These results might suggest that the position effect observed here was not dependent on the inserted transgene. It should be noted that about as much as a 50-fold more virus stock solution of Z-E3R vector could be needed than that of the Z-E1L vector to obtain the same expression level, because the titer of Z-E3R vector was about one-tenth and the expression level obtained was about one-fifth when the same volume of the virus stock solution is used for infection (Figure 2a, bars 7 and 10; Figure 5b, bars 2–5 and 8–11). We also measured the expressed protein levels of GFP and LacZ using fluorometry and β-galactosidase assay, respectively (Figure 6a and b). The G-E1 vectors produced significantly more GFP than the G-E4 vectors (Figure 6a, bars 2 and 3 to 6 and 7; bars 8 and 9 to 12 and 13), although the G-E3L vector expressed a similar level to that of the G-E1 vectors (bars 4 and 10). Also, the Z-E1 vectors expressed more LacZ than the Z-E3 and Z-E4 vectors (Figure 6b, bars 2 and 3 to 4–7; bars 8 and 9 to 10–13). These results in respect of the protein level confirm the mRNA expression levels measured by qPCR shown in Figure 5a and b.

To examine whether the position effects may also be observed for a tissue-specific promoter and for genes other than GFP and LacZ, the HuH-7 cells were infected with the vector expressing Cre under the control of the AFP promoter and the Cre expression levels were measured. The AFP promoter is specifically active in the HuH-7 cells derived from hepatocarcinoma in contrast to the case in the 293 cells. Because tissue-specific promoters, including the AFP promoter, are generally weak, the expressed Cre mRNA level was too low to measure quantitatively. Therefore, we used the method of 'excisional expression,' where the Cre enzyme driven by the AFP promoter switched on the potent EF1α promoter and specifically enhanced the expression level of dsRed by about 50-fold[17] (the strategy is shown in Supplementary Figure S1). The results were again very similar to those obtained using the EF1α promoter (Figure 6a and b): the AFP-E3 and E4 vectors expressed only about a half to one-fifth of dsRed mRNA than the AFP-E1 vectors (Figure 5c, bars 3 and 4 to 5–8, 9 and 10 to 11–14). Therefore, although the vector titers obtained using the AFP promoter were not influenced by their insertion sites (Figure 2b), the position effects at the E1, E3 and E4 sites showed very similar patterns to those of the EF1α promoter. Altogether, the E3L/R and E4L/R vectors expressed about two to fivefold less transgene products than the E1L/R vectors, not only when the potent EF1α promoter was used, but also when the tissue-specific AFP promoter was used, suggesting there may be a mechanism common to these promoters.

To examine whether the position effect of expression observed in the HuH-7 cells may also be observed in other cells, the HeLa cells were infected with the GFP-expressing vectors at MOI 3 and at MOI 10 (Figure 7a and b). The G-E1L vector expressed a significantly greater amount of mRNA than the G-E3 and G-E4 vectors (Figure 7a, bars 2 to 4, 6 and 7; bars 8 to 10, 12 and 13). However, the mRNA level of the E1R vector was not significantly different from those of the E3 and E4 vectors, because the

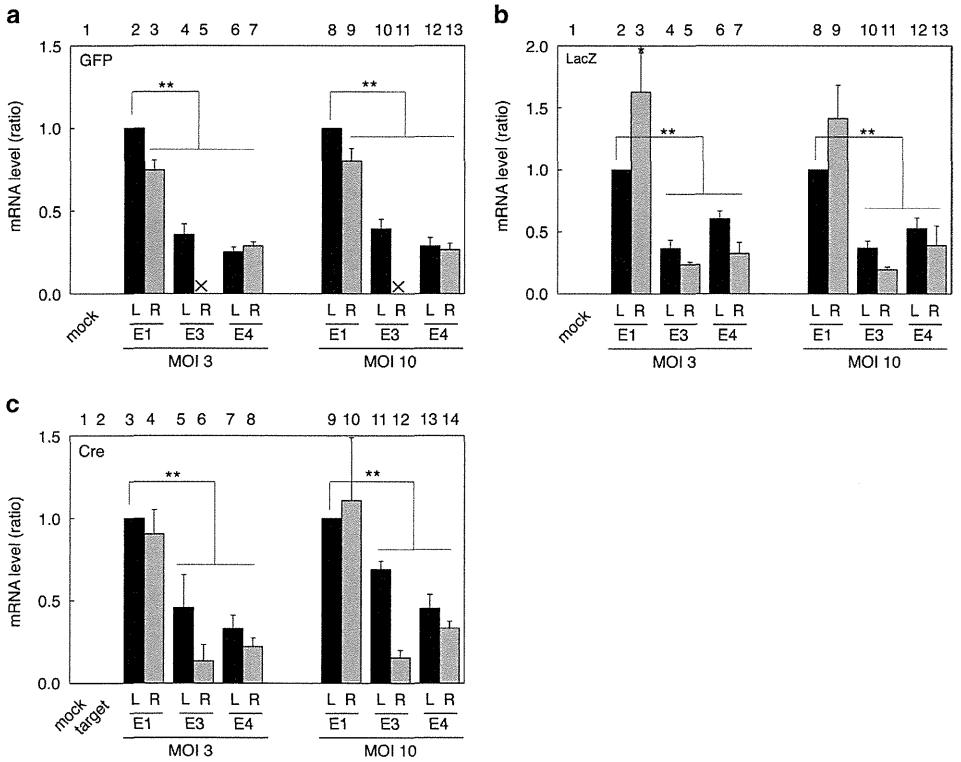

Figure 5. Expression levels of the transgene mRNA in the infected HuH-7 cells. The mRNA levels are shown relative to the mRNA level of the transgene in E1L-infected cells set as 1. (**a**) GFP mRNA levels. The cells were infected with the EF-GFP AdVs at the indicated MOIs. The GFP mRNA levels were quantified by qPCR, $n=3$. (**b**) LacZ mRNA levels. The cells were infected with the EF-LacZ AdVs. LacZ mRNA levels are shown in the same manner as that described in (**a**), $n=4$. (**c**) Cre mRNAs levels. The cells were co-infected with the AFP-Cre AdVs (switch vectors) and a target vector which expressed dsRed by Cre-mediated recombination (excisional expression). The dsRed mRNA levels were quantified in the same manner as that described in (**a**), $n=6$. Error bars indicate mean ± s.d; mock, HuH-7 cells without infection; target, HuH-7 cells infected with the target vector only; $^{*}P<0.05$, $^{**}P<0.01$. The other representations are the same as those in Figure 1.

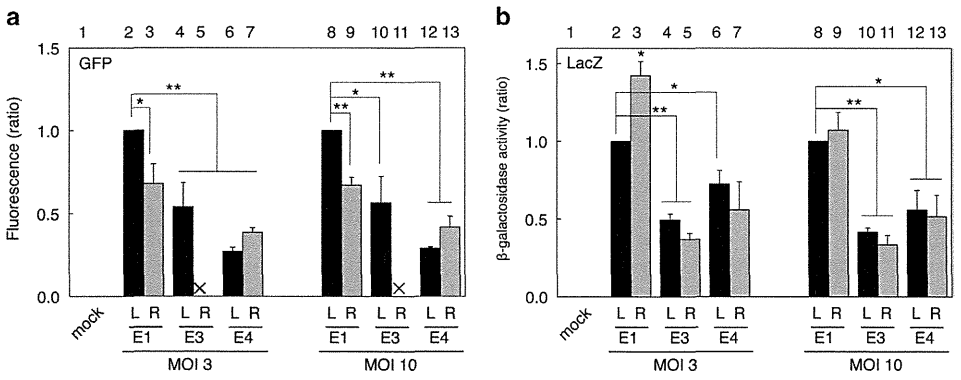

Figure 6. Protein expression levels in the infected HuH-7 cells. (**a**) Fluorescence of GFP. The cells were infected with the EF-GFP AdVs at the indicated MOIs. The fluorescence of GFP was quantified by Ascent fluorometry. The fluorescences are shown relative to the fluorescence level in E1L-infected cells set as 1, $n=4$. (**b**) Activities of β-galactosidase. The cells were infected with the EF-LacZ AdVs. β-galactosidase activities were evaluated by the β-gal assay, $n=3$. Error bars represent ± s.d.; mock, mock infection of HuH-7 cells; $^{*}P<0.05$, $^{**}P<0.01$. The other representations are the same as those in Figure 1.

expressed mRNA level of the E1R was lower than that of the E1L (bars 3 to 4, 6 and 7; bars 9 to 10, 12 and 13). Similar results were obtained using GFP fluorometry: the G-E1L vector exhibited significantly more fluorescence than the other G-E3 and G-E4 vectors (Figure 7b, bars 2 to 4, 6 and 7), whereas the E1R vector expression was not statistically significant (bars 3 to 4, 6 and 7). These results were confirmed by fluorescence microscopy (Supplementary Figure S2a). Moreover, the same results were obtained using the CV-1 cell line derived from monkey fibroblasts (Supplementary Figure S2b). Therefore, very similar position effect

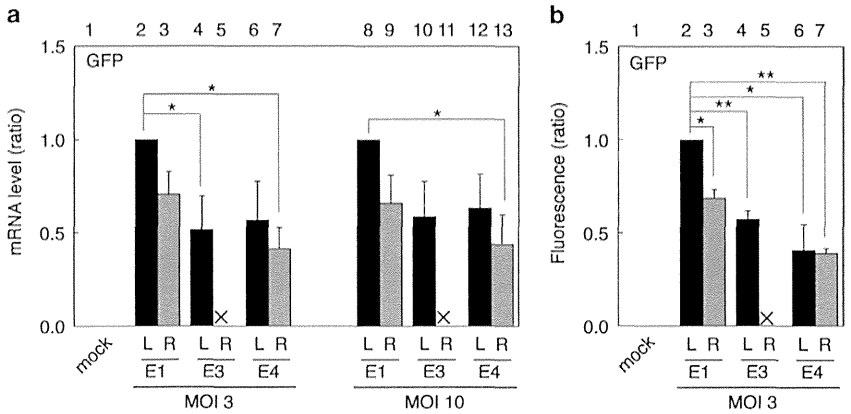

Figure 7. Expression levels of the transgene mRNA and protein in the infected HeLa cells. (**a**) GFP mRNA levels. The HeLa cells were infected with the EF-GFP AdVs at the indicated MOIs. The other representations are the same as those in Figure 4a, $n=3$. (**b**) Fluorescence of GFP. The HeLa cells were infected with EF-GFP AdVs at MOI 3. The other representations are the same as those in Figure 5a, $n=4$. Error bars indicate mean ± s.d.; mock, mock infection of HeLa cells; $^{*}P < 0.05$, $^{**}P < 0.01$.

among the E1, E3 and E4 insertion sites are obtained at least for the G-E1L vector.

DISCUSSION

We demonstrated in this study that the inserted sites and orientations for a given transgene greatly influenced the vector titers and expression levels. Especially, when the transgene was inserted in E3R, the GFP-expressing vector could not be obtained and the LacZ-expressing vector titer was extremely low. Also, the titer of E3L AdV was lower than that of E1L AdV. Because the aberrantly spliced mRNAs from the transgenes to a viral gene have been reported for the E1R site/orientation[15] (described below), and similar aberrant splicing might have occurred for E4L site/orientation in the same mechanism. Therefore, considering the titers, aberrant splicing and expression levels, E1L and E4R sites/orientations were preferable for the main target gene and the second gene, respectively, in the simultaneous expression. As for the titer, the information might be useful not only for FG AdVs but also for the replication-competent AdVs containing E1A gene under the control of a cancer-specific promoter, because they both are prepared using the 293 cells.

We have demonstrated that the vectors containing transgene at E1L/R showed higher titers and expression levels than other vectors. E1L/R is the most frequently used, probably because the E1 site is required or convenient for the major methods of AdV construction which are now commonly used.[18–20] For example, for the method established by the Graham's group, the use of the E1 site is essential because it exploits the viral packaging sequences partially overlapping with the E1 region. Consequently, we think that the E1 site, found to be the best in this work, might have been chosen in the currently popular methods. However, there seems to be one concern with E1R: aberrant splicing has been reported to occur to viral pIX gene from the cryptic donors present not only in the LacZ gene but also in the herpes thymidine-kinase (TK) gene, which is used for positron emission tomography as a reporter gene and for suicide gene therapy. Consequently, TK-pIX and LacZ-pIX fusion proteins were produced, and the pIX protein evokes strong immune responses.[15] For this reason, we always adopt the leftward orientation for the E1 site.

Currently, in the simultaneous expression of the target gene and the reporter gene, the E3 sites are mostly employed for the reporter gene.[21–25] However, as described here, when the LacZ-expressing transgene driven by the EF1α promoter was inserted at E3R, the vector titer and expression level were very low, probably because of the aberrant splicing, and the G-E3R AdV could not be obtained. In our experiences, the E3R AdV containing GFP gene driven by SRα promoter[26] could also not be obtained. In contrast, however, the E3R AdV containing GFP driven by CMV promoter could be obtained. The reason of such difference is unclear, but it might be related to the fact that both EF1α and SRα promoters contain the splicing unit including the splicing acceptor site in their promoters, which might produce the aberrant mRNA spliced from the MLP donor, but the CMV promoter contain no splicing unit. Because aberrant splicing was detected even at E3L, both E3R and E3L were problematic and to be avoided, if possible.

The E4 site has not frequently been used.[17,19,27–29] The E4 insertion position, *Sna*BI site, is located 162 nucleotides (nt) from the right end of the AdV genome. Vectors containing a transgene at the E4 site showed high titers, although their expression levels were lower than those of the E1 vectors. The titers and expression levels do not significantly differ between E4L and E4R vectors. However, the E4L might produce aberrantly spliced mRNAs as observed for the E3L/R. The E4R site/orientation was successfully used as the position of the second transgene[17] where Cre was expressed under the control of the AFP promoter. The expressed Cre turned on the potent promoter present at the E1L and the high-level expression of the target gene was obtained, while maintaining strict sepecificity. Interestingly, it was also recently reported that the E4L, not the E4R, is better than the E1 site for short hairpin RNA expression.[27] The difference may be related to the use of the RNA polymerase III promoter for the short hairpin RNA production, whereas the polymerase II promoter is used for the protein production. If so, the E4L may be advantageous not only for the production of short hairpin RNA, but also of guide RNAs used for the CRISPR/Cas9 system.[30,31] The reported results might not contradict with the results described here, because the RNA polymerase III expression is not involved with splicing.

Altogether, therefore, the E1L and E4R sites/orientations appear to be the best for use in AdVs for the simultaneous expression of the target gene and reporter gene, respectively. Importantly, the occurrence of aberrant splicing sometimes yields a viral-transgene fusion protein, which may induce strong immune responses caused by the viral encoding region.[15] The probability is one-third to coincide the coding frame of the transgene with that of the viral gene. The coding regions of the four aberrant mRNAs described in this report were, by chance, connected out-of-frame, yielding no transgene-fusion protein, but only a truncated LacZ protein composed of several amino acids. However, in a previous study,[15] LacZ-pIX and TK-pIX fusion proteins were produced under the control of potent promoters. Thus, the production of such fusion proteins by aberrant splicing is not a rare event.

In general, use of the same promoter may cause troubles by the homologous recombination in the simultaneous recombination. We have experienced that, when the identical promoters in the E1L and E4R sites/orientations were applied, a rearrangement through the homologous recombination occurred, whereas the AdVs in the E1L and E4L was stable. Therefore, use of different promoters would be preferable.

The harmful aberrant splicing can be avoided using the technique described herein. The aberrant splicing can be identified by PCR analysis as reported here. The preferred sequences of the splicing donor site are AGGT/AAGT (slash denotes the exon-intron junction), where the underlined GT dinucleotides are definitely required for splicing. Nucleotide mutations of these sequences, especially the GT nucleotides, can be introduced without changing the amino acid encoded by the therapeutic gene, and successful disruption of the aberrant splicing can be easily confirmed by a subsequent PCR using the same primer set. As an example, the change from T to C, G or T (Gly) in the aberrant splicing present in the TK gene removes the splicing while keeping the amino acid sequence intact, and this mutated TK gene is expected to be safer than the original TK gene for suicide gene therapy and for positron emission tomography analyses using TK gene as a reporter.

The results described here demonstrated that position effects were evident for the expression of transgenes present on the AdV genome. The mechanisms of the position effect in the AdV genome are unknown. We think that viral enhancers, silencers or other *cis*-acting sequences near to the foreign transgene promoter might influence its expression. It might be related to the fact that similar results were obtained for a strong EF1α promoter and a cancer-specific AFP promoter. In contrast to the expression levels, the vector titers were probably not influenced by the position of the transgene, because similar and high titers were obtained using a tissue-specific promoter, which does not produce the transgene mRNA in the 293 cells (Figure 2b). The results might suggest that the vector titers were mainly influenced by the combination of a strong promoter and aberrant splicing between the transgene and viral genes (Figure 2a). These results are probably valuable for efficient and safe gene therapy using FG AdVs.

In this work, the range of the E3 deletion is between two *Xba*I sites in the E3 region (nt position 28,592–30,470). Because the lengths of the E3 deletions are slightly different among the commercially available AdV construction kits, the differences might influence the results obtained here. We surmise that these differences might not influence the conclusion described here as far as the same transgene is used, because the same splicing event is essentially expected to occur by the same mechanism. However, the possibility cannot be ruled out.

The cassette plasmids (also used as cosmids) are available on request in a collaboration basis, which bear the full-length AdV genome containing the unique *Swa*I site at the E1 site and the unique *Cla*I site at the E4 site (pAxw4cit2) and that inversely containing the *Cla*I site at the E1 site and *Swa*I at the E4 site (pAxc4wit2). The method to insert a transgene into these sites is described in the Materials and Methods section.

MATERIALS AND METHODS

Cells and virus titration

Human 293,[32] HeLa and HuH-7 cell lines are derived from the human embryonic kidney, human cervical carcinoma and human hepatocellular carcinoma, respectively. The CV-1 cell line is derived from African green monkey kidney. The cells were cultured in Dulbecco's Modified Eagles Medium supplemented with 10% fetal calf serum. The 293 cells constitutively express adenoviral E1 genes and support the replication of E1-substituted AdVs. After infection with AdVs, the cells were maintained in Dulbecco's Modified Eagles Medium supplemented with 5% fetal calf serum without geneticin. FG AdVs were titrated using the method described by Pei *et al.*[16] Briefly, the copy numbers of a viral genome that was successfully transduced into the infected target cells were measured by real-time PCR (relative virus titer). HuH-7 cells were used as the target cells. The titer of the standard virus was determined using the copy number of serially diluted plasmid DNA. When FG AdVs are used, the relative virus titer (copies per ml) normally corresponds to about one-fifth of the Tissue Culture Infectious Dose 50 titer, when the gene product is not deleterious; the probable reason for this difference is that the transduction efficiency of the 293 cells is exceptionally high as compared with that of the other cells. The sequences of the TaqMan probes for the titration are derived from adenovirus-5 (Ad5) pIX gene: forward primer, 5′-TGTG ATGGGCTCCAGCATT-3′; probe, 5′-ATGGTCGCCCCGTCCTGCC-3′; reverse primer, 5′-TCGTAGGTCAAGGTAGTAGAGTTTGC-3′.

Vector construction

All the AdVs described here were constructed using the cosmid cassette pAxcwit2 containing the full-length AdV genome.[19,33] The GFP/LacZ-expression unit were under the control of the EF1α promoter[34] and the Cre-expression unit was driven by the AFP promoter; the AFP promoter used here was the (AB) 2S6 AFP promoter.[35] All the expression units were inserted into the *Swa*I cloning site at the E1 substitution region as E1L or R vectors. All the E3L and E3R vectors possessed the same expression units at the *Xba*I site in the E3 region of pAxcwit2; the *Xba*I site is originally generated by deletion between the two *Xba*I sites in the Ad5 genome (nt position 28,592-30,470). The E4 cloning site represented by the *Sna*BI site (nt position 35770) located in the E4 region at 165-nt downstream from the right end of the Ad5 genome.[17]

Conventional PCR

The PCR experiments were essentially performed by the standard method.[36] Typically, the 293 cells in the 6-well plate were infected at MOI 5 and 16 h post infection, total RNAs were prepared and reverse-transcribed using oligo(dT) primer; the resultant cDNAs were amplified by PCR with Tks Gflex DNA polymerase (Takara Bio, Shiga, Japan) and a PCR system (ProFlex PCR system, Applied Biosystems, Foster City, CA, USA). The PCR cycling conditions were in accordance with the manufacturer's protocol (Takara Bio): 94 °C for 1 min, followed by 30 cycles at 98 °C for 10 s, 60 °C for 15 s, and 68 °C for 30 s. The primer sets are described in Supplementary Table S2. The PCR products containing each splice junction were subjected to agarose gel electrophoresis.

Quantitative real-time PCR

The sequences of the GFP primers and the dsRed primers have been described previously.[17,37] The sequences of the LacZ primers were as follows: forward primer, 5′-ATCAGGATATGTGGCGGATGA-3′; probe, 5′-CGG CATTTTCCGTGACGTCT-3′; reverse primer, 5′-TGATTTGTGTAGTCGGTTTA TGCA-3′. The primer sequences of the normal splicing junctions of MLP-fiber and MLP-hexon were as follows: for MLP-fiber detection forward primer in MLP third exon, 5′-AAAGGCGTCTAACCAGTCACAGT-3′; probe in the fiber gene, 5′-AGCGCGAAGACCGTCTGAAGATACC-3′; reverse in the fiber gene, 5′-CCGCTTTCCGTGTCATATGG-3′; and for MLP-hexon detection forward primer in MLP third exon, 5′-TCTAACCAGTCACAGTCGCAAGA-3′; probe in the hexon gene, 5′-CGCGCCCGCTTTCCAAGATG-3′; reverse in the hexon gene, 5′-CACTGCGGCATCATCGAA-3′.

The mRNA levels were calculated as described by Maekawa *et al.*[37] Briefly, the total RNA of the infected cells was extracted, and the amounts of the expressed target RNAs and 18S-rRNA (correction standard) were quantified using reverse transcription (TaqMan Reverse Transcription Reagents, Roche, Basel, Switzerland) and real-time PCR (Applied Biosystems Prism 7000); the ratio of the target RNA to 18S-rRNA was then calculated. To quantify the AdV genome, the infected total cell DNA was prepared from the cells using a previously described method[29,38] or a DNA preparation kit (Macherey-Nagel, through Takara Bio). Quantitative PCR was performed to detect the AdV genome using a probe for the pIX gene, as described above.[17] The amount of chromosomal DNA was simultaneously measured to correct the Ct values of the viral genome per cell, and the corrected Ct is shown throughout. The probes were derived from the sequence of the human β-actin gene for the HeLa and HuH7 cell lines. The qPCR reaction was performed using the following cycling conditions according to the manufacturer's protocol (Applied BioSystems): 50 °C for 2 min and 95 °C for 10 min, followed by 40 cycles at 95 °C for 15 s and 60 °C for 1 min.

Measurement of the expressed GFP and LacZ

The HuH-7, HeLa and CV1 cells were infected at MOI 3 or MOI 10 of each vector in a 24-well plate in triplicated experiments. Three days after the infection, the infected cells were washed twice with phosphate-buffered saline.The cells in the three wells were then fixed with 4% paraformaldehyde to quantify the GFP fluorescence using Labsystems Fluoroskan Ascent FL (GMI, Ramsey, MN, USA) or by fluorescence microscopy. The cells infected with the LacZ vectors were harvested for the quantification of β-galactosidase (β-gal) (β-gal assay kit, Invitrogen, Carlsbad, CA, USA). To quantify the β-gal activity, the infected cells were disrupted by sonication and the lysate was subjected to a color reaction assay using o-Nitrophenyl β-D-galactopyranoside. The stained color standard was determined using 5-bromo-4-chloro-3-indolyl-β-D-galactopyranoside (X-gal).

Insertion of a transgene into the cassette plasmid (cosmid) containing both the E1 and E4 sites

The method of inserting a given transgene into the *Swa*I site of pAxw4cit2 and pAxc4wit2 is followed by the protocol of Takara Bio (Adenovirus Dual Expression Kit). Briefly, the plasmid containing the transgene DNA fragment is treated with the appropriate restriction enzymes and treated with the DNA polymerase I Klenow fragment, followed by agarose gel electrophoresis. The isolated transgene fragment of about 50 ng is ligated with 1–2 μg of the cassette cosmid at a volume of 15 μl at 15 °C for overnight. The ligated DNA is cleaved with *Swa*I to remove the self-ligated parent plasmid, and then transformation or lambda *in vitro* packaging is performed. The latter method is highly efficient and removes the deleted plasmids smaller than 38 kb. To insert a given transgene DNA to the *Cla*I site, the DNA fragment is treated with the Klenow polymerase and ligated with a DNA linker of *Bsp*T104I (Takara Bio, reaction temperature is 37 °C) or *Bst*BI (New England Biolabs, Ipswich, MA, USA, 65 °C), 5′-GGTTCGAACC-3′ (the underline shows the recognition sequences), for example, and digested with either enzyme. Because the termini produced with this enzyme can be ligated with *Cla*I-cleaved DNA and the ligated DNA cannot be cleaved with either enzyme. Therefore, after ligation of the transgene and *Cla*I-cleaved cassette, the self-ligated parent plasmid can be removed by *Cla*I digestion. Alternatively, both *Swa*I and *Cla*I sites can be converted to I-*Ceu*I, I-*Sse*I or both by insertion of the cleavage-site oligonucleotides.

CONFLICT OF INTEREST

The authors declare no conflict of interest.

ACKNOWLEDGEMENTS

We thank N Goda for research assistance and Ms T Shino for her secretarial assistance. This study was supported in part by Grants-in-Aids from the Ministry of Education, Culture, Sports, Science and Technology to YK and SK; The Program for Intractable Disease Research utilizing Disease-specific iPS Cells from JST to YK; a grant for Practical Research on Hepatitis B (009) from the Ministry of Health, Labour and Welfare of Japan to IS.

REFERENCES

1 Crystal RG. Adenovirus: the first effective in vivo gene delivery vector. *Hum Gene Ther* 2014; **25**: 3–11.
2 Watanabe M, Nasu Y, Kumon H. Adenovirus-mediated REIC/Dkk-3 gene therapy: Development of an autologous cancer vaccination therapy (Review). *Oncol Lett* 2014; **7**: 595–601.
3 Wold WS, Toth K. Adenovirus vectors for gene therapy, vaccination and cancer gene therapy. *Curr Gene Ther* 2013; **13**: 421–433.
4 Danthinne X, Imperiale MJ. Production of first generation adenovirus vectors: a review. *Gene Ther* 2000; **7**: 1707–1714.
5 Gil JS, Machado HB, Campbell DO, McCracken M, Radu C, Witte ON *et al.* Application of a rapid, simple, and accurate adenovirus-based method to compare PET reporter gene/PET reporter probe systems. *Mol Imaging Biol* 2013; **15**: 273–281.
6 Qin C, Lan X, He J, Xia X, Tian Y, Pei Z *et al.* An in vitro and in vivo evaluation of a reporter gene/probe system hERL/(18)F-FES. *PloS One* 2013; **8**: e61911.
7 Zhang G, Lan X, Yen TC, Chen Q, Pei Z, Qin C *et al.* Therapeutic gene expression in transduced mesenchymal stem cells can be monitored using a reporter gene. *Nucl Med Biol* 2012; **39**: 1243–1250.
8 Gambhir SS, Barrio JR, Phelps ME, Iyer M, Namavari M, Satyamurthy N *et al.* Imaging adenoviral-directed reporter gene expression in living animals with positron emission tomography. *Proc Natl Acad Sci USA* 1999; **96**: 2333–2338.
9 Chan HY, V S, Xing X, Kraus P, Yap SP, Ng P *et al.* Comparison of IRES and F2A-based locus-specific multicistronic expression in stable mouse lines. *Plos One* 2011; **6**: e28885.
10 Kim JH, Lee SR, Li LH, Park HJ, Park JH, Lee KY *et al.* High cleavage efficiency of a 2A peptide derived from porcine teschovirus-1 in human cell lines, zebrafish and mice. *Plos One* 2011; **6**: e18556.
11 Small JC, Kurupati RK, Zhou X, Bian A, Chi E, Li Y *et al.* Construction and characterization of E1- and E3-deleted adenovirus vectors expressing two antigens from two separate expression cassettes. *Hum Gene Ther* 2014; **25**: 328–338.
12 Pham L, Nakamura T, Gabriela Rosales A, Carlson SK, Bailey KR, Peng KW *et al.* Concordant activity of transgene expression cassettes inserted into E1, E3 and E4 cloning sites in the adenovirus genome. *J Gene Med* 2009; **11**: 197–206.
13 Yankulov K. Dynamics and stability: epigenetic conversions in position effect variegation. *Biochem Cell Biol* 2013; **91**: 6–13.
14 Wilson C, Bellen HJ, Gehring WJ. Position effects on eukaryotic gene expression. *Annu Rev Cell Biol* 1990; **6**: 679–714.
15 Nakai M, Komiya K, Murata M, Kimura T, Kanaoka M, Kanegae Y *et al.* Expression of pIX gene induced by transgene promoter: possible cause of host immune response in first-generation adenoviral vectors. *Hum Gene Ther* 2007; **18**: 925–936.
16 Pei Z, Kondo S, Kanegae Y, Saito I. Copy number of adenoviral vector genome transduced into target cells can be measured using quantitative PCR: Application to vector titration. *Biochem Biophys Res Commun* 2012; **417**: 945–950.
17 Kanegae Y, Terashima M, Kondo S, Fukuda H, Maekawa A, Pei Z *et al.* High-level expression by tissue/cancer-specific promoter with strict specificity using a single-adenoviral vector. *Nucleic Acids Res* 2011; **39**: e7.
18 Bett AJ, Haddara W, Prevec L, Graham FL. An efficient and flexible system for construction of adenovirus vectors with insertions or deletions in early regions 1 and 3. *Proc Natl Acad Sci USA* 1994; **91**: 8802–8806.
19 Miyake S, Makimura M, Kanegae Y, Harada S, Sato Y, Takamori K *et al.* Efficient generation of recombinant adenoviruses using adenovirus DNA-terminal protein complex and a cosmid bearing the full-length virus genome. *Proc Natl Acad Sci USA* 1996; **93**: 1320–1324.
20 Mizuguchi H, Kay MA. Efficient construction of a recombinant adenovirus vector by an improved in vitro ligation method. *Hum Gene Ther* 1998; **9**: 2577–2583.
21 Shin SP, Seo HH, Shin JH, Park HB, Lim DP, Eom HS *et al.* Adenovirus Expressing Both Thymidine Kinase and Soluble PD1 Enhances Antitumor Immunity by Strengthening CD8 T-cell Response. *Mol Ther* 2013; **21**: 688–695.
22 Suzuki T, Sasaki T, Yano K, Sakurai F, Kawabata K, Kondoh M *et al.* Development of a recombinant adenovirus vector production system free of replication-competent adenovirus by utilizing a packaging size limit of the viral genome. *Virus Res* 2011; **158**: 154–160.
23 Trujillo MA, Oneal MJ, McDonough S, Qin R, Morris JC. A probasin promoter, conditionallfor exampley replicating adenovirus that expresses the sodium iodide symporter (NIS) for radiovirotherapy of prostate cancer. *Gene Ther* 2010; **17**: 1325–1332.
24 Mailly L, Boulade-Ladame C, Orfanoudakis G, Deryckere F. A novel adenovirus vector for easy cloning in the E3 region downstream of the CMV promoter. *Virol J* 2008; **5**: 73.
25 Mizuguchi H, Kay MA, Hayakawa T. In vitro ligation-based cloning of foreign DNAs into the E3 and E1 deletion regions for generation of recombinant adenovirus vectors. *Biotechniques* 2001; **30**: 1112–1114; 1116.
26 Takebe Y, Seiki M, Fujisawa J, Hoy P, Yokota K, Arai K *et al.* SR alpha promoter: an efficient and versatile mammalian cDNA expression system composed of the simian virus 40 early promoter and the R-U5 segment of human T-cell leukemia virus type 1 long terminal repeat. *Mol Cellular Biol* 1988; **8**: 466–472.
27 Pei Z, Shi G, Kondo S, Ito M, Maekawa A, Suzuki M *et al.* Adenovirus vectors lacking virus-associated RNA expression enhance shRNA activity to suppress hepatitis C virus replication. *Sci Rep* 2013; **3**: 3575.
28 Mizuguchi H, Xu ZL, Sakurai F, Mayumi T, Hayakawa T. Tight positive regulation of transgene expression by a single adenovirus vector containing the rtTA and tTS expression cassettes in separate genome regions. *Hum Gene Ther* 2003; **14**: 1265–1277.
29 Saito I, Oya Y, Yamamoto K, Yuasa T, Shimojo H. Construction of nondefective adenovirus type 5 bearing a 2.8-kilobase hepatitis B virus DNA near the right end of its genome. *J Virol* 1985; **54**: 711–719.
30 Cong L, Ran FA, Cox D, Lin SL, Barretto R, Habib N *et al.* Multiplex genome engineering using CRISPR/Cas systems. *Science* 2013; **339**: 819–823.
31 Mali P, Yang LH, Esvelt KM, Aach J, Guell M, DiCarlo JE *et al.* RNA-guided human genome engineering via Cas9. *Science* 2013; **339**: 823–826.

32 Graham FL, Smiley J, Russell WC, Nairn R. Characteristics of a human cell line transformed by DNA from human adenovirus type 5. *J Gen Virol* 1977; **36**: 59–74.

33 Fukuda H, Terashima M, Koshikawa M, Kanegae Y, Saito I. Possible mechanism of adenovirus generation from a cloned viral genome tagged with nucleotides at its ends. *Microbiol Immunol* 2006; **50**: 643–654.

34 Kim DW, Uetsuki T, Kaziro Y, Yamaguchi N, Sugano S. Use of the human elongation factor-1-alpha promoter as a versatile and efficient expression system. *Gene* 1990; **91**: 217–223.

35 Sato Y, Tanaka K, Lee G, Kanegae Y, Sakai Y, Kaneko S *et al.* Enhanced and specific gene expression via tissue-specific production of Cre recombinase using adenovirus vector. *Biochem Biophys Res Commun* 1998; **244**: 455–462.

36 Sambrook J, Russell DW. *Molecular Cloning: a laboratory manual*, 3rd edn. Cold Spring Harbor Laboratory Press: Cold Spring Harbor, New York, 2001.

37 Maekawa A, Pei Z, Suzuki M, Fukuda H, Ono Y, Kondo S *et al.* Efficient production of adenovirus vector lacking genes of virus-associated RNAs that disturb cellular RNAi machinery. *Sci Rep* 2013; **3**: 1136.

38 Nakano M, Odaka K, Takahashi Y, Ishimura M, Saito I, Kanegae Y. Production of viral vectors using recombinase-mediated cassette exchange. *Nucleic Acids Res* 2005; **33**: e76.

Supplementary Information accompanies this paper on Gene Therapy website (http://www.nature.com/gt)

OPEN ACCESS Freely available online

PLOS ONE

Adenovirus-Encoding Virus-Associated RNAs Suppress HDGF Gene Expression to Support Efficient Viral Replication

Saki Kondo[1], Kenji Yoshida[2], Mariko Suzuki[1], Izumu Saito[1], Yumi Kanegae[1]*

1 Laboratory of Molecular Genetics, Institute of Medical Science, University of Tokyo, Shirokanedai, Minato-ku, Tokyo, Japan, **2** Regenerative and Cellular Medicine Office, Sumitomo Dainippon Pharma Co., Ltd., Minatojima Minamimachi, Chuo-ku, Kobe, Japan

Abstract

Non-coding small RNAs are involved in many physiological responses including viral life cycles. Adenovirus-encoding small RNAs, known as virus-associated RNAs (VA RNAs), are transcribed throughout the replication process in the host cells, and their transcript levels depend on the copy numbers of the viral genome. Therefore, VA RNAs are abundant in infected cells after genome replication, i.e. during the late phase of viral infection. Their function during the late phase is the inhibition of interferon-inducible protein kinase R (PKR) activity to prevent antiviral responses; recently, mivaRNAs, the microRNAs processed from VA RNAs, have been reported to inhibit cellular gene expression. Although VA RNA transcription starts during the early phase, little is known about its function. The reason may be because much smaller amount of VA RNAs are transcribed during the early phase than the late phase. In this study, we applied replication-deficient adenovirus vectors (AdVs) and novel AdVs lacking VA RNA genes to analyze the expression changes in cellular genes mediated by VA RNAs using microarray analysis. AdVs are suitable to examine the function of VA RNAs during the early phase, since they constitutively express VA RNAs but do not replicate except in 293 cells. We found that the expression level of hepatoma-derived growth factor (HDGF) significantly decreased in response to the VA RNAs under replication-deficient condition, and this suppression was also observed during the early phase under replication-competent conditions. The suppression was independent of mivaRNA-induced downregulation, suggesting that the function of VA RNAs during the early phase differs from that during the late phase. Notably, overexpression of HDGF inhibited AdV growth. This is the first report to show the function, in part, of VA RNAs during the early phase that may be contribute to efficient viral growth.

Citation: Kondo S, Yoshida K, Suzuki M, Saito I, Kanegae Y (2014) Adenovirus-Encoding Virus-Associated RNAs Suppress HDGF Gene Expression to Support Efficient Viral Replication. PLoS ONE 9(10): e108627. doi:10.1371/journal.pone.0108627

Editor: Motoyuki Otsuka, The University of Tokyo, Japan

Received July 29, 2014; **Accepted** September 2, 2014; **Published** October 2, 2014

Data Availability: The authors confirm that all data underlying the findings are fully available without restriction. All relevant data except for the microarray data are within the paper and its Supporting Information files. All the data acquired by the microarray analysis were deposited in the NCBI Gene Expression Omnibus (NO. GSE58605).

Funding: This work was supported in part by Grants-in-Aid from the Ministry of Education, Culture, Sports, Science and Technology (http://www.jsps.go.jp/english/index.html) to S.K. and Y.K. and the Ministry of Health, Labour and Welfare (http://www.mhlw.go.jp/english/index.html) for Research on the Innovative Development and the Practical Application of New Drugs for Hepatitis B to I.S. This work was supported in part by the Program for Intractable Disease Research utilizing Disease-specific iPS Cells from JST to Y.K. The funders had no role in study design, data collection and analysis, decision to publish, or preparation of the manuscript.

Competing Interests: The authors of this manuscript have the following competing interests: K. Yoshida is employed by Dainippon Sumitomo Pharma Co., Ltd. This does not alter the authors' adherence to PLOS ONE policies on sharing data and materials.

* Email: kanegae@ims.u-tokyo.ac.jp

Introduction

It has become increasingly clear over the past decade that non-coding small RNAs play roles in viral life cycles at various ways [1–3]. Hepatitis C virus (HCV) is known to utilize host microRNA miR122, which is specifically expressed and highly abundant in the human liver, to support its efficient replication through its direct attachment to the HCV 5′ non-translation region; thus, miR122 is regarded as a therapeutic target for antiviral intervention [4–6]. Moreover, more than two hundred small RNAs derived from viruses have been identified. For example, Epstein-Barr virus (EBV) encodes two small RNAs, EBER-1 and EBER-2 [7–9], which modulate the interferon-mediated antiviral response [10].

Adenoviruses (Ads) encode two kinds of non-coding small-RNAs, known as virus-associated (VA) RNAs, VAI and VAII, that consist of 157–160 nucleotides (nts). After Ad infection, the transcription of VA RNAs starts at the same time as the E1A gene and lasts until the late phase. Since the transcription level of VA RNAs increases depending on the number of viral genome copies, VA RNAs in Ad-infected cells are abundant during the late phase, and this is one reason why the functional analysis of VA RNAs during the late phase has been investigated much more frequently than during the early phase.

The VA RNA I (VAI), which is expressed at a level of 10^8 copies per infected cell during the late phase [11], is required to establish efficient translation in virus-infected cells [12,13]. Moreover, it is well known that VAI inhibits anti-viral double-stranded RNA (dsRNA)-activated protein kinase (PKR). Also, VAI stabilizes ribosome-associated viral mRNAs, which could lead to enhanced levels of protein synthesis [14]. These findings have indicated that VAI plays a role in creating suitable conditions for viral growth, at

least during the late phase of infection. Recently, VA RNAs have been reported to be processed to microRNAs (mivaRNAs) via the cellular RNA-interference (RNAi) machinery, and mivaRNAs disturb cellular DNA expressions during the late phase [15]. However, it has not been investigated the function of VA RNA during the early phase, though the expression of VA RNAs starts immediately during the early phase of viral infection.

E1- and E3-deleted adenovirus vectors (AdVs), known as first-generation (FG) AdVs, have widely been used for the transient expression of transgenes in various cell types. FG AdVs lack E1A gene, an essential for viral replication; consequently, they neither express any viral gene product in target cells nor replicate except in 293 cells, which express E1A gene constitutively. However, since VA RNAs are transcribed by RNA polymerase III, their expressions are independent of E1A-mediated transactivation and they are always transcribed from AdV genome in AdV-infected cells. Therefore, FG AdVs are thought to be a suitable tool for the investigation of VA RNA function during the early phase of viral infection, since they express VA RNAs but do not replicate except in 293 cells. Moreover, these AdVs allow us to study the function of VA RNAs during both early and late phase using 293 cells. For this purpose, AdVs lacking VA RNA genes (VA-deleted AdVs) are essential as a control; however, VA-deleted AdVs have been difficult to generate and produce in quantities sufficient for practical use. Recently, we have developed a novel method for the efficient production of VA-deleted AdVs using a site-specific recombinase FLP [16]. A "pre-vector" containing the VA RNA region flanked by a pair of FRT sequences, which are target sequences for FLP recombinase, is constructed according to a commonly used method for the production of FG AdV [17]. This pre-vector, which is obtained at a high titer, is subsequently used to infect a 293 cell line that constitutively expresses humanized-FLPe [18] (293hde12) [19] so that the VA RNA region is removed from replicating viral genome. Since the excision efficiency of FLP in 293hde12 cells is high enough to remove almost all the VA RNA region from the very high number of viral genome copies, this method can be used to generate a high-titer of VA-deleted AdVs efficiently.

Here, we demonstrated the effect of VA RNAs expressed via FG AdVs on cellular gene expression by comparing the expression patterns between VA-deleted AdV- and FG AdV-infected cells using a microarray analysis. We found that VA RNAs expressed from FG AdVs disturbed the cellular gene expressions. Especially, the expression level of HDGF (hepatoma-derived growth factor; ENSG00000143321.14) was significantly decreased under the replication-deficient conditions; notably, HDGF expression started to decrease even during the early phase of infection in the 293 cells. Moreover, the overexpression of the HDGF gene inhibited viral growth in 293 cells, suggesting that the suppression of HDGF gene expression mediated by the VA RNAs was important for viral growth. This is the first report to show the function of VA RNAs during the early phase of infection.

Materials and Methods

Cells and AdVs

Human embryo kidney 293 cell line (ATCC) [20], human lung carcinoma A549 cell line (ATCC) [21], and human hepatocellular carcinoma derived HuH-7 cell line (RIKEN BRC) [22]were cultured in Dulbecco's modified Eagle's medium (DMEM) supplemented with 10% fetal calf serum (FCS). 293hde12 cell line [19], which is a 293 cell line possessing the hFLPe gene [18] (an improved version of the FLPe gene [23]), was cultured in DMEM supplemented with 10% FCS plus geneticin (0.75 mg/mL). After infection with AdVs, the cells were maintained in DMEM supplemented with 5% FCS without geneticin. For AraC (cytosine b-D-arabinofuranoside, hydrochloride: Sigma) treatment, the infected cells were maintained in DMEM supplemented with 5% FCS plus AraC (20 μg/mL).

The FG AdVs were prepared using 293 cells, which constitutively express adenoviral E1 genes and support the replication of E1-substituted AdVs. The VA-deleted AdVs except for HDGF- and GFP-expressing AdVs were prepared according to a method using 293U6VA-1 cells that constitutively express both VAI and VAII. HDGF-expressing and GFP-expressing VA-deleted AdVs were generated as described previously [16]. Briefly, an HDGF-expressing and a GFP-expressing unit under the control of the EF1α promoter was inserted into the SwaI cloning site at the authentic E1 substitution region in the pre-vector cosmid pAxdV-4FVF-w, and the pre-vectors were prepared using 293 cells. Subsequently, the pre-vectors were used to infect 293hde12 cells that constitutively express humanized FLPe recombinase [19] to excise the VA RNA region from the replicating viral genome. The VA-deleted AdVs transcribed less than 1% of the VA RNAs, compared with the FG AdVs, as confirmed using real-time PCR [16]. The VA-deleted AdVs and the FG AdVs were titrated using the methods described by Pei et al [24]. Briefly, the copy numbers of a viral genome that was successfully transduced into infected target cells were measured using qPCR (relative virus titer: rVT). This method enabled us to compare the various titers, since the transduction titer is not influenced by the growth rate of the 293 cells, even if an expressed gene product is deleterious to 293 cells.

Plasmids

The pVA41da plasmid [16] contains a DNA fragment covering all of VAI and VAII from nt position 10576–11034 of adenovirus type 5. The pBluescript SK (-) (Stratagene) was used as a control. The plasmids were transfected using Transfast (Promega). A pxEFGFP plasmid expressing GFP under the control of the EF1α promoter was used as a transfection control. Two days after the transfection of pVA41da plasmid into 293 cells, the cells were harvested and the total RNAs were extracted as described below to measure the HDGF mRNA levels using qPCR.

Microarray analysis

VA-deleted AdV (Axd12CARedE) and VA-containing FG AdV (AxCAdsRedE) were infected at an MOI (multiplicity of infection) of 0.5 to A549 cells for 24 h. We prepared triplicate samples for each of the conditions, and total RNA isolation was performed using a Qiagen RNeasy kit (Qiagen). A DNA microarray analysis using Affymetrix Gene-Chip technology was performed as described previously [25–27]. Briefly, 100 ng of total RNAs were used as a template for cDNA synthesis, and biotin-labeled cRNA was synthesized with a 3′ IVT Express Kit (Affymetrix). After generating the hybridization cocktails, hybridization to the DNA microarray (Genechip; Human Genome U133 Plus 2.0 Array; Affymetrix) [28] and fluorescent labeling were performed. The microarrays were then scanned with a GeneChip; Scanner 3000 7G System (Affymetrix). The data analysis was performed using GCOS software (Affymetrix). Signal detection and quantification were performed using the MAS5 algorithm with default settings. Global normalization was performed so that the average signal intensity of all the probe sets was equal to 100. For the clustering analysis, the signals were normalized and calculated to the individual scores, and the scores were visualized using Spotfire DecisionCite [29]. The analysis of variance among the groups was also performed using Spotfire DecisionCite and normalized data.

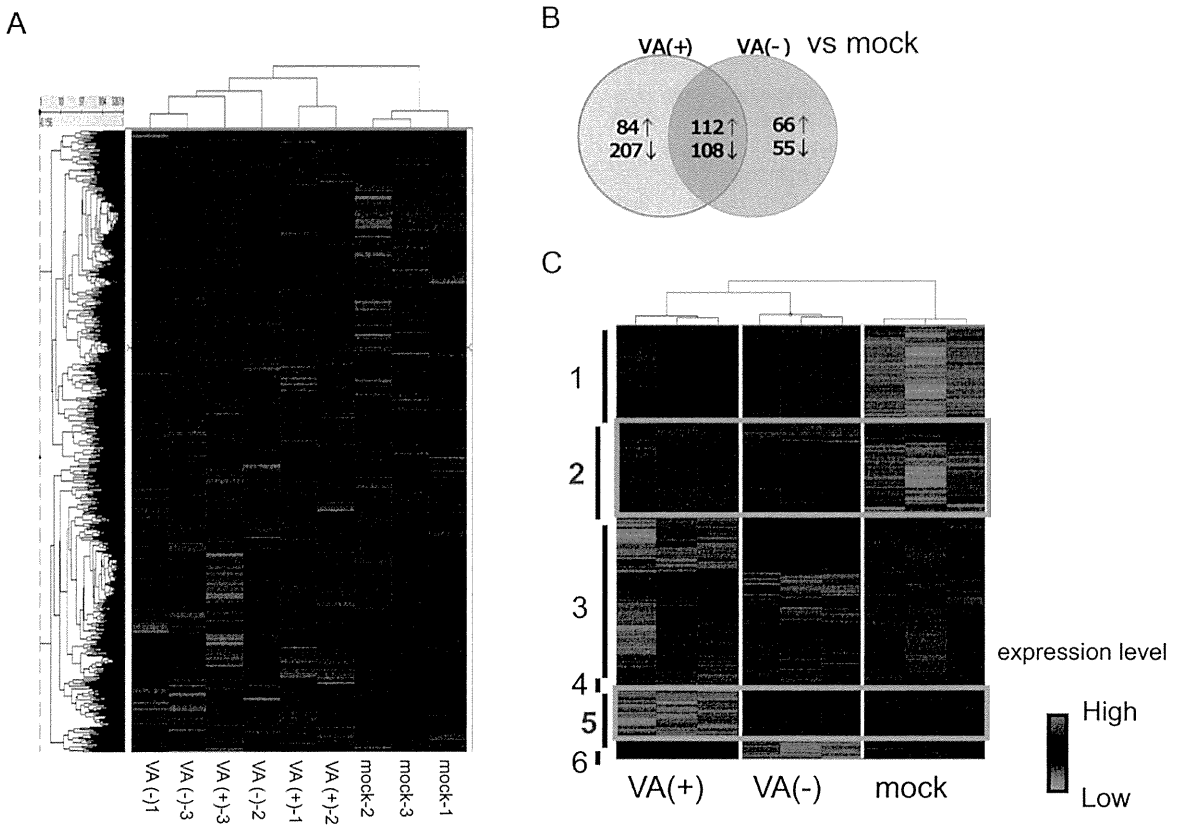

Figure 1. Microarray analysis. Global gene expression analysis of AdV infected A549 cells by Affymetrix microarray. Cells were harvested and total RNA was isolated after 24 h after infection. (A) Hierarchical clustering analysis using 32,619 genes of which expression was determined as "Present" in GCOS software in every sample. (B) The numbers of up or down regulated genes compared with mock infected group (Fold change >1.5, $P<0.01$). Red arrow indicates the numbers of up-regulated genes, and blue arrow indicates the numbers of down-regulated genes. (C) Identification and isolation of VA (+) specific gene clusters by hierarchical clustering analysis. The numbers of target genes were 2,800 genes, which were selected by ANOVA analysis in advance.
doi:10.1371/journal.pone.0108627.g001

All the data acquired by the microarray analysis were deposited in the NCBI Gene Expression Omnibus (NO. GSE58605).

Quantitative real-time PCR

The total RNA of the infected cells was extracted, and the amount of expressed target RNA and 18S-rRNA (correction standard) were quantified using reverse-transcription and real-time PCR (Applied Biosystems Villa7); the ratio of the target RNA to 18S-rRNA was then calculated. To quantify the AdV genome, the infected total cell DNA was prepared from cells using a previously described method [30,31] or a DNA preparation kit (TaKaRa Bio). Quantitative PCR (qPCR) was performed to detect the AdV genome using a probe for the pIX gene, as described previously [24]. The amount of chromosomal DNA was simultaneously measured to correct the Ct values of the viral genome per cell. The probes were derived from the sequence of the human β-actin gene for HeLa and HuH-7 cell lines. The qPCR reaction was performed according to the manufacturer's protocol: 50°C for 2 min and 95°C for 10 min, followed by 40 cycles of 95°C for 15 sec and 60°C for 1 min (Applied BioSystems).

Western blot analysis

Two days after transfection, 293 cells were harvested and the total protein was extracted using NP-40 lysis buffer [50 mM Tris-HCl (pH 8.0), 0.15M NaCl, 5 mM EDTA, 1% NP-40]. The lysates were mixed well in a rotator for 2 h at 4°C, centrifuged at 15,000 rpm for 5 min at 4°C, and the supernatants were collected. Western blotting was performed as described previously [32]. The membrane was incubated for 2 h at room temperature in the presence of anti-HDGF mouse monoclonal antibody (Bio Matrix Research, #BMR00572) diluted to 0.3 μg/mL with PBS-Tween, followed by incubation with peroxidase-conjugated goat anti-mouse IgG+IgM (Jackson Immunoresearch, #115-035-068) diluted to 1/10,000 with PBS-Tween. An anti-actin peptide goat polyclonal antibody (Santa Cruz Biotechnology, #sc-1616) diluted to 1/200 was also detected to show equal loading.

Results

HDGF gene expression was downregulated in FG-AdV infected cells

To determine whether VA RNAs expressed from FG AdVs disturb cellular gene expression, a microarray analysis was performed. We conducted a hierarchical clustering analysis using data for 32,619 genes, which were determined by GCOS software as being expressed in all the samples. The clusters were divided into two clear groups: namely, a mock group and an AdV-infected group (Figure 1A). Then, we conducted a pairwise comparison and drew a Venn diagram between the mock group vs. VA (−), i.e. VA-deleted AdV, and the mock group vs. VA (+), i.e. FG AdV,

according to the criteria of a 1.5-fold change (either an increase or a decrease) and $P<0.01$. In AdV-infected cells, more than 600 genes showed a significant increase/decrease against the mock cells in total. The numbers of VA-(+) specific genes and VA-(−) specific genes were found to be 300 and 100, respectively (Figure 1B). These results indicated that the VA RNAs expressed from AdV do not have a major impact on the expressions of whole genes. Using an ANOVA analysis ($P<0.01$) and a hierarchical clustering analysis, we isolated 6 gene clusters and 2,800 genes that showed different gene expressions between any of the group combinations. Among the 6 clusters, gene clusters 2 and 5 exhibited VA (+)-specific increases in gene expression and VA (+)-specific decreases in gene expression, respectively. According to this gene list (Table S1 in File S1) and literature survey, we finally selected several genes as targets for further research.

Next, we attempted to validate whether our microarray strategy was actually capable of identifying the targets of VA RNAs. We selected a subset of genes, all of which were upregulated or downregulated only after FG AdV infection and not after VA-deleted AdV infection, compared with the mock cells, and measured their transcript levels using quantitative RT-PCR (qPCR) in HeLa cells and HuH-7 cells. The results showed that the expression levels of some of these selected genes were actually changed in response to VA RNAs in both cell lines, except for the PTPRJ gene (Table 1). In contrast, we did not observe any significant changes in the transcript levels of TIA-1 (ENSG00000116001.11), which have been identified as a target for mivaRNA, a microRNA derived from VA RNA [15]. We chose the HDGF gene for further analysis since its transcript was remarkably decreased in both cell lines when FG AdVs were infected.

HDGF gene expression was suppressed by a lower level of VA RNAs than TIA-1

To examine whether the VA RNAs expressed from a plasmid also suppress HDGF gene expression, a VA-RNA expressing-plasmid, pVA41da [16], was transfected into 293 cells. Two days later, the total cellular RNA and protein were collected and HDGF expression was measured at the transcript level using qPCR (Figure 2A) and at the protein level using a western blot analysis (Figure 2B), respectively. The result showed that HDGF mRNA was significantly decreased, even in cells with a low level of VA-RNA transduction (Figure 2A, HDGF, 0.1 μg/well), in comparison with control plasmid-transduced cells (Figure 2A, HDGF, 0). In contrast, no significant change in TIA-1 expression was observed in the low VA RNA transduced cells (Figure 2A, TIA-1, 0.1 and 0.25), and it was suppressed only in the highest VA RNA-transduced cells (Figure 2A, TIA-1, 0.5). HDGF suppression mediated by VA RNA was also detected at the protein level (Figure 2B). The HDGF protein was significantly decreased in cells that had been transfected with the VA RNA-expressing plasmid (Figure 2B, lane 2, VA (+)), compared with the mock cells (lane 1, mock) or the control plasmid-transduced cells (lane 3, VA (−)). The suppression of HDGF transcript was also observed in VA RNA-expressing 293 cell lines named 293VA1 and 293VA42 [33], compared with that in the parent 293 cells (Table S2 in File S1). Therefore, VA RNAs suppressed HDGF expression under the conditions other than viral infection, and a smaller amount of VA RNA than TIA-1 was sufficient to suppress HDGF.

HDGF gene expression was suppressed during the early phase of viral infection

To determine the period during which HDGF was downregulated in the adenovirus life cycle, the VA-deleted AdVs and the FG-AdVs were used to infect 293 cells at an MOI of 5. Then, the cellular RNA was isolated to measure the HDGF transcript levels using qPCR at the indicated time points (Figure 3). The VA-deleted AdVs and the FG-AdVs are structurally identical except for their VA RNA expression, and these E1-deleted vectors are able to replicate in 293 cells because the E1 proteins are supplied *in trans*. The results showed that the transcript levels of HDGF started to decrease at 8 h after infection (early phase) in FG AdV-infected cells (Figure 3A, white circle). Interestingly, after VA-deleted AdV infection, the HDGF level clearly increased above the basal level at 8 h (Figure 3A, black square). This induction of HDGF expression after VA-deleted AdV infection was also observed under replication-deficient conditions in HuH-7 cells (Figure S1 in File S1, bars 1 and 3). In contrast, the TIA-1 mRNA level was similar to the basal level at 8 h and it obviously decreased to comparable level with HDGF only at 16 h (late phase) after FG-AdV infection (Figure 3B, white circle), whereas no significant upregulation was observed after VA-deleted AdV infection (Figure 3B, black square). Since the replication of the viral genome occurs at around 8 h after infection, these results showed that the suppression of HDGF and TIA-1 began during the early and late phases of viral infection, respectively. The results for TIA-1 suppression using AdVs were consistent with those of a previous report indicating that TIA-1 is downregulated during the late phase of infection with wild-type adenovirus [15]. We further examined the point that the HDGF level increased to more than 125% of the steady-state level at 8 h after VA-deleted AdV infection (Figure 3A), though the TIA-1 level did not (Figure 3B).

Table 1. Changes in expression levels of cellular genes in response to VA RNAs.

gene	ratio VA(+)/VA(−)	
	HuH-7	HeLa
PAPPA	1.23	1.60
PTPRJ	1.09	1.06
STS1-3	0.82	0.80
HDGF	0.43	0.65
TIA-1	1.10	1.09

Each mRNA level in the HuH-7 cells and HeLa cells was quantified using qPCR, and the ratio of the expression level in FG AdV infected cells (VA (+)) compared with that in VA-deleted AdV infected cells (VA (−)) was calculated.

doi:10.1371/journal.pone.0108627.t001

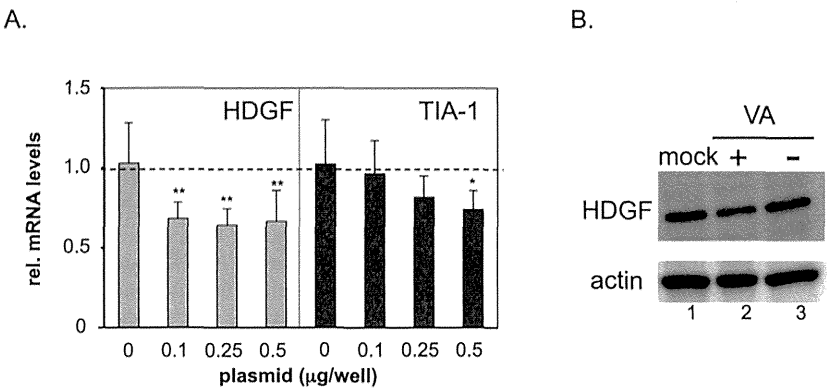

Figure 2. HDGF is downregulated in the presence of VA RNA. (A) HDGF and TIA-1 mRNA levels after VA RNA-expressing plasmid (pVAda41) transfection. RNA (A) and protein (B) were isolated after 48 h from 293 cells transfected with pVA41da or control plasmid. HDGF or TIA-1 and 18S rRNA were quantified using qPCR and plotted for comparison. The expression level in control-plasmid transfected cells was set at 1, and the ratio of the expression levels in all the cases was calculated. The error bars show the standard deviations of three different experiments. *$P<0.05$, **$P<0.01$ compared with mock cells (unpaired Student *t*-test). (B) HDGF and actin, used as a loading control, were evaluated using western blot analysis.
doi:10.1371/journal.pone.0108627.g002

VA RNAs suppressed the upregulation of HDGF gene expression during the early phase of viral infection

Although the replication of AdV genome starts 8 h after infection, the possibility that the infected cells at 8 h might contain cells reaching late phase cannot be ruled out. To examine the change in HDGF gene expression strictly during the early phase, VA-deleted and FG AdV-infected 293 cells were treated with AraC (cytosine β-D-arabinofuranosde hydrochloride), a nucleoside analog. AraC inhibits viral DNA replication and the transition from the early phase to the late phase; thus, AraC treatment amplifies the effect during the early phase. After the isolation of cellular RNA at 8 h and 24 h after infection, the transcript level of each gene was measured using qPCR and the relative mRNA level of each gene against the steady state level was calculated (Figure 4). The levels of both transcripts in AraC-treated cells at 8 h (white bars) was expected to be similar to those in untreated cells, since the replication of the viral genome had not yet started at this time point regardless of AraC treatment. Remarkably, the induction of HDGF after VA-deleted AdV infection against uninfected cells was detected at much higher levels at 24 h (bar 2) than at 8 h (bar 1). Since AraC amplifies the effect during the early phase, this result confirmed that HDGF gene expression is induced during the early phase of infection. Furthermore, after FG AdV infection with AraC treatment, no significant suppression was observed even at 24 h (bar 4), although without AraC the HDGF level was obviously decreased (Figure 3A, white circle). This result suggested that the increase in HDGF is offset by VA RNAs at 24 h in the presence of AraC, and the amount of VA RNA is not sufficient to decrease this high HDGF level below the basal level. In contrast, no significant change was observed in the TIA-1 level after VA-deleted AdV infection in AraC-treated cells (bars 5 and 6) and at 8 h after FG AdV infection (bar 7), as expected. However, the TIA-1 level was decreased at 24 h after FG AdV infection even in AraC-treated cells (bar 8), though AraC treatment inhibits transition to the late phase. The reason for this observation is unknown, but the amount of accumulated VA RNA might be sufficient for processing to mivaRNAs to suppress TIA-1 expression, which was not increased after AdV infection. Although VA RNAs suppressed both HDGF and TIA-1, the results shown here suggested that the suppression mechanism mediated by VA RNA is different from each other.

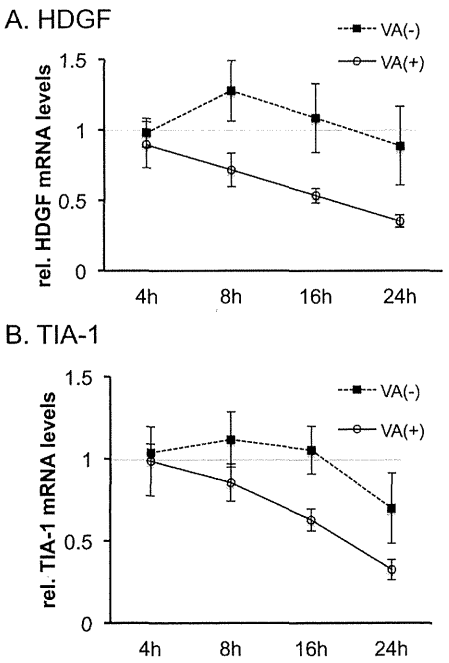

Figure 3. Suppression of HDGF begins during the early phase of viral infection. RNA was isolated from 293 cells infected with VA-deleted AdV (VA (−)) or FG AdV (VA (+)) after the indicated time periods. HDGF (A) and TIA-1 (B) mRNAs were quantified using qPCR. The expression level in uninfected cells was set at 1, and the ratio of the expression level in all the cases was calculated. The error bars show the standard deviations of three different experiments.
doi:10.1371/journal.pone.0108627.g003

Overexpression of HDGF gene inhibited VA-deleted AdV replication

Since the expression of the HDGF gene was increased after VA-deleted AdV infection during the early phase and, therefore, VA RNAs seemed to be responsible for the suppression of the increase in HDGF, we wondered whether HDGF affects viral growth. To test this hypothesis, HDGF-expressing VA-deleted AdVs and FG AdVs were constructed and used to infect 293 cells; the growth

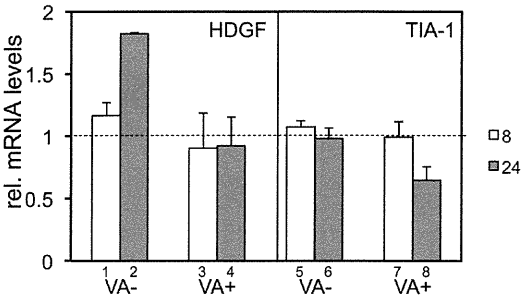

Figure 4. HDGF is upregulated during the early phase of viral infection in VA-deleted AdV-infected 293 cells. RNA was isolated from AraC-treated 293 cells infected with VA-deleted AdV (VA (−)) or FG AdV (VA (+)) after 8 h (white bars) and 24 h (gray bars), and each mRNA level was quantified using qPCR. The expression level in uninfected cells was set at 1, and the ratio of the expression level in all the cases was calculated. The error bars show the standard deviations of three different experiments.
doi:10.1371/journal.pone.0108627.g004

efficiency of each AdV was then determined using qPCR to measure the viral genome copy number (Figure 5). We applied an efficient method of generating the VA-deleted AdVs using a site-specific recombinase FLP [16]. A pre-vector, which contains VA RNA genes flanked with a pair of FRTs that are target sequences of FLP, was generated in 293 cells because it behaves as the same as FG AdVs. Subsequently, an obtained pre-vector with a high titer was used to infect 293hde12 cells [19], which are 293 cells expressing the humanized FLPe gene, to excise VA RNA genes out from the replicating AdV genome. For the efficient production of VA-deleted AdVs, a pre-vector was infected five-times more than for FG-AdV production. Under this condition, all cells are infected at once (one-step infection), and the amount of VA RNAs expressed from a pre-vector is sufficient to support the generation of HDGF-expressing VA-deleted AdVs. After AdV infection, the HDGF gene on the AdV genome is expressed exogenously under the control of a potent EF1α promoter. Therefore, the amount of HDGF protein is probably much higher than the endogenous level during AdV replication in 293 cells.

Each vector was used to infect 293 cells at an MOI of 0.5 and the infected cells were collected after 1 to 4 days. GFP-expressing AdV was used as a control. In this infection condition, only a

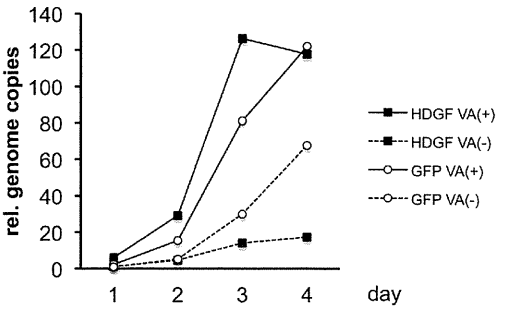

Figure 5. AdV growth in 293 cells. Total DNA was isolated from VA-deleted AdVs (VA (−)) or FG AdVs (VA (+)) infected 293 cells and each AdV genome copy was quantified using qPCR. The level of AdV genome in 293 cells after infection with GFP-expressing FG AdV on day1 was set at 1, and the ratio of the expression level in all the cases was calculated. Three independent experiments were carried out and representative results are shown.
doi:10.1371/journal.pone.0108627.g005

fraction of cells are infected and the uninfected cells are further infected by the newly produced AdVs (multistep infection). Although the growth of HDGF-expressing and GFP-expressing VA-deleted AdVs (dotted lines) was significantly lower than those of FG AdVs (solid lines), this finding was consistent with previous studies indicating a positive role of VA RNAs in viral growth [16,34]. The results clearly showed that the overexpression of the HDGF gene did not inhibit FG-AdV growth in comparison with control-FG AdV (solid lines). However, the growth of HDGF-expressing VA-deleted AdVs, the genome of which was only amplified to 20 copies on day 4, was much lower than that of GFP-expressing VA-deleted AdVs (dotted lines), which reached 70 copies. These results showed that the overexpression of the HDGF gene inhibited AdV replication as far as HDGF was not suppressed by VA RNAs.

Discussion

In this study, we demonstrated that adenovirus encoding VA RNAs suppressed HDGF gene expression. This finding revealed, for the first time, a partial role of VA RNAs in the early phase of viral infection.

The suppression of the HDGF level was observed even in cells infected with replication-deficient FG AdVs, which express a much smaller amount of VA RNAs than replicating viruses. The suppression was also detected during the early phase of viral infection in the AdV replication system, i.e., at 8 h after FG AdV infection in 293 cells. In contrast, we confirmed that TIA-1, which is suppressed by VA RNAs during the late phase of viral infection as reported by Aparicio *et al.* [15], was decreased only when VA RNAs were abundant or during the late phase of infection. Although both of these two genes, HDGF and TIA-1, were suppressed in response to VA RNAs, we revealed that the suppression of HDGF required a much smaller amount of VA RNAs than the suppression of TIA-1. This result led us to conclude that VA RNAs probably have different functions during each phase through the regulation of different gene expressions.

According to the adenovirus life cycle, the expression of E1A gene, which is a transactivator for DNA-polymerase II-dependent viral early-gene expression, starts in the immediately during the early phase. The transcription of VA RNAs mediated by DNA polymerase III is independent of E1A-regulated transcription and, therefore, starts almost at the same time as E1A. The amount of VA RNAs during the early phase is much lower than that during the late phase, since it depends on the number of genome copies, which increases to 100,000 copies per cell in the late phase. Actually, the level of VA RNAs during the early phase was about 200-times lower than that during the late phase (Table S3 in File S1). Therefore, the amount of VA RNAs expressed from replication-deficient FG-AdVs is also much smaller than that during the late phase of viral infection. It has been reported that VA RNAs are processed to microRNAs (mivaRNAs) through cellular RNAi machinery and that knockdown of Dicer using siRNA promotes the growth of VA-deleted adenoviruses [35]. However, mivaRNAs suppress TIA-1 expression only during the late phase [15] and have never been detected during the early phase of viral infection [34,36]. These findings strongly suggest that VA RNAs are processed to microRNAs only when the VA RNAs are abundant. Therefore, the suppression of HDGF gene expression by VA RNAs may not due to mivaRNAs.

In fact, our reporter assay using luciferase suggested that HDGF may not a target for mivaRNAs (Figure S2 in File S1). There is a putative target sequence for a mivaRNA in the 3′ UTR region of the HDGF gene, and we examined whether it is a target sequence

or not. As a result, no significant reduction in luciferase activity was detected when the putative seed sequence was cloned into the downstream of luciferase gene. The result suggested that, at least, the known mivaRNAs are not responsible for HDGF suppression. Together with the results shown in Figure 2 and 4, this finding indicated that the role of VA RNAs during the early phase differs from that during the late phase of viral infection, although further investigation is required to reveal the HDGF suppression mechanism mediated by VA RNAs.

The fact that the amount of VA RNA required for HDGF suppression differs from that required for TIA-1 suppression may explain why our microarray analysis did not detect the TIA-1 gene as a positive target. Aparicio *et al.* used cells transfected with a VA RNA-expressing plasmid for their microarray analysis [15]; however, it is difficult to introduce the same number of plasmid copies into 100% of the cells uniformly. Therefore, the results for cells with a high-copy number of plasmids, rather than those for cells with a low-copy number of plasmids, might be favored if a cell mixture containing both high-copy and low-copy number of plasmids is used for the microarray analysis. Consequently, they identified TIA-1 as a target of mivaRNA. In contrast, our microarray using AdVs for VA RNA transduction enabled us to introduce a small amount of VA RNAs into all the cells present in the dish in a uniform manner [18], allowing us to identify novel target genes of VA RNAs during the early phase of infection.

The E1A gene is essential for the adenovirus life cycle and viruses cannot replicate without E1A, such as AdV, which lacks the E1 genes and replicates only in E1-expressing 293 cells. Recently, the interaction of E1A with a cellular factor, CtBP (transcriptional corepressor C-terminal binding protein), has been reported to be required for the efficient E1A-mediated transactivation of early genes [37]. CtBP was initially discovered during screening for cellular factors binding to, and modulating the activity of E1A protein in Ras-mediated tumorigenesis [38]. CtBP was subsequently shown to play an important role in the regulation of cellular genes involved in growth and differentiation [39]. The C-terminal region of E1A interacts with CtBP, and an adenovirus containing the E1A mutation within the CtBP-binding motif, PLDLS, has been shown to decrease the level of early gene expression and, consequently, to inhibit viral growth.

HDGF has also been reported to be a CtBP-binding protein. Yang and Everett showed that HDGF functions as a transcriptional repressor of the SET and MYND domain containing 1 (SMYD1) gene through its interaction with CtBP using the same binding site as E1A [40]. HDGF is a transcription factor consisting of a nuclear protein with both mitogenic and angiogenic activity that is highly expressed in the developing heart and vasculature. HDGF contains an N-terminal PWWP domain and a C-terminal NLS signal. HDGF interacts with CtBP through a non-canonical binding motif (PKDLF), which is located within the PWWP domain, and represses target gene expression by binding to the promoter region leading to cell proliferation. Since both the HDGF and E1A proteins utilize the same binding site on the N-terminus of CtBP using PXDLS-like motifs [40,41], HDGF might compete with E1A to interact with CtBP. In other words, adenovirus may suppress the expression of HDGF, a cellular-CtBP binding protein, using VA RNAs so that E1A acquires an advantage for CtBP binding.

Our results showed that the upregulation of HDGF, compared with the steady-state level, was observed after infection with VA-deleted AdVs both during the early phase of the replicating condition and during replication-deficient conditions. Of note, some of other CtBP-binding proteins were also transcriptionally upregulated under the same conditions resulting in HDGF upregulation, and VA RNA suppressed these gene expressions, although the expression changes in these genes were not as noticeable as that of HDGF (Table S4 in File S1). These findings suggest that VA RNAs selectively suppress the induction in gene expressions, resulting in the expression of CtBP-binding proteins that may play a role in competitive inhibition with the E1A-CtBP interaction. Moreover, VA RNAs suppress the expression of these genes before the replication of the viral genome, i.e., during the early phase, because E1A-CtBP functions during this phase [37]. In other words, VA RNAs may act to prevent one of the host-defense mechanisms that lead to the inhibition of E1A function, which is essential for the initiation of viral replication.

In the case of AdV infection at a low MOI, which is similar to the condition for native viral infection, the growth of HDGF-expressing VA-deleted AdVs was much lower than that for GFP-expressing VA-deleted AdVs as well as FG AdVs (Figure 5). This result indicates that HDGF expression inhibits viral growth only when the replication starts from a small amount of virus. Our study using AdV at a low MOI may reflect actual viral infection during the very early phase, since a target cell does not express E1A protein before infection and viral infection does not occur at a high MOI. From this point of view, the suppression of the expression of CtBP-binding proteins mediated by VA RNAs might be advantageous for viral growth.

The E1- and E3-deleted AdVs used in this study are widely applied for various studies including gene therapy. However, this vector has two concerns. One is that it, in fact, expresses viral genes, pIX and VA RNAs. It is known that AdVs cause severe immune responses, and we have reported that a main cause is aberrant expression of immunogenic, viral pIX protein, and the pIX protein is not produced when EF1α promoter is used for transgene expression [42]. In terms of VA RNAs, it has not been clear whether a small amount of VA RNAs transcribed via AdVs affects physiological responses in the infected cells or not. The study described here is the first report to show that the VA RNAs expressed from AdVs disturb cellular gene expressions including a transcription factor, HDGF. Our results strongly suggest that production of VA RNAs would be avoided, if possible, when AdVs are applied for gene therapy, since VA RNAs expressed from FG AdVs may affect various cellular signaling pathways. Disturbance of cellular gene expression caused by VA RNAs might also affect the data in the basic study using AdVs. Moreover, although AdVs are often applied for shRNA expression, VA RNA expressed from AdVs inhibits shRNA activity [33], since VA RNAs utilize cellular RNAi machinery for processing of mivaRNAs. The present study provided further evidence that VA-deleted AdVs are useful and might be substituted for FG AdVs.

Supporting Information

File S1 **Figure S1**, HDGF is suppressed after FG AdV infection in HuH-7 cells. **Figure S2**, HDGF mRNA is not a direct target of mivaRNAI-138. **Table S1**, Gene list for gene clusters 2 and 5. **Table S2**, HDGF and TIA-1 expression levels in 293 cell lines. **Table S3**, Amount of VA RNAs after FG AdV infection in 293 cells. **Table S4**, Ratio of expression levels of genes known to be CtBP-binding proteins after AdV infection in HuH-7 cells.
(PPT)

Acknowledgments

We thank Ms. T. Shiino for her secretarial assistance and A. Maekawa and M. Yamasaki for critical readings of our manuscript, and Dr. Hiroyuki Nakagawa for assistance of microarray analysis.

Author Contributions

Conceived and designed the experiments: SK YK IS. Performed the experiments: SK KY MS. Analyzed the data: SK KY. Contributed reagents/materials/analysis tools: SK YK. Wrote the paper: SK YK IS.

References

1. Grundhoff A, Sullivan CS (2011) Virus-encoded microRNAs. Virology 411: 325–343.
2. Zhou R, Rana TM (2013) RNA-based mechanisms regulating host-virus interactions. Immunol Rev 253: 97–111.
3. Narayanan A, Kehn-Hall K, Bailey C, Kashanchi F (2011) Analysis of the roles of HIV-derived microRNAs. Expert Opin Biol Ther 11: 17–29.
4. Pedersen IM, Cheng G, Wieland S, Volinia S, Croce CM, et al. (2007) Interferon modulation of cellular microRNAs as an antiviral mechanism. Nature 449: 919–922.
5. Jopling CL, Yi M, Lancaster AM, Lemon SM, Sarnow P (2005) Modulation of hepatitis C virus RNA abundance by a liver-specific MicroRNA. Science 309: 1577–1581.
6. Fukuhara T, Matsuura Y (2013) Role of miR-122 and lipid metabolism in HCV infection. J Gastroenterol 48: 169–176.
7. Bornkamm GW (2009) Epstein-Barr virus and its role in the pathogenesis of Burkitt's lymphoma: an unresolved issue. Semin Cancer Biol 19: 351–365.
8. Lerner MR, Andrews NC, Miller G, Steitz JA (1981) Two small RNAs encoded by Epstein-Barr virus and complexed with protein are precipitated by antibodies from patients with systemic lupus erythematosus. Proc Natl Acad Sci U S A 78: 805–809.
9. Yajima M, Kanda T, Takada K (2005) Critical role of Epstein-Barr Virus (EBV)-encoded RNA in efficient EBV-induced B-lymphocyte growth transformation. J Virol 79: 4298–4307.
10. Greifenegger N, Jager M, Kunz-Schughart LA, Wolf H, Schwarzmann F (1998) Epstein-Barr virus small RNA (EBER) genes: differential regulation during lytic viral replication. J Virol 72: 9323–9328.
11. Mathews MB (1995) Structure, function, and evolution of adenovirus virus-associated RNAs. Curr Top Microbiol Immunol 199 (Pt 2): 173–187.
12. Schneider RJ, Weinberger C, Shenk T (1984) Adenovirus VAI RNA facilitates the initiation of translation in virus-infected cells. Cell 37: 291–298.
13. Reichel PA, Merrick WC, Siekierka J, Mathews MB (1985) Regulation of a protein synthesis initiation factor by adenovirus virus-associated RNA. Nature 313: 196–200.
14. O'Malley RP, Duncan RF, Hershey JW, Mathews MB (1989) Modification of protein synthesis initiation factors and the shut-off of host protein synthesis in adenovirus-infected cells. Virology 168: 112–118.
15. Aparicio O, Carnero E, Abad X, Razquin N, Guruceaga E, et al. (2010) Adenovirus VA RNA-derived miRNAs target cellular genes involved in cell growth, gene expression and DNA repair. Nucleic Acids Res 38: 750–763.
16. Maekawa A, Pei Z, Suzuki M, Fukuda H, Ono Y, et al. (2013) Efficient production of adenovirus vector lacking genes of virus-associated RNAs that disturb cellular RNAi machinery. Sci Rep 3: 1136.
17. Fukuda H, Terashima M, Koshikawa M, Kanegae Y, Saito I (2006) Possible mechanism of adenovirus generation from a cloned viral genome tagged with nucleotides at its ends. Microbiol Immunol 50: 643–654.
18. Kondo S, Takata Y, Nakano M, Saito I, Kanegae Y (2009) Activities of various FLP recombinases expressed by adenovirus vectors in mammalian cells. J Mol Biol 390: 221–230.
19. Takata Y, Kondo S, Goda N, Kanegae Y, Saito I (2011) Comparison of efficiency between FLPe and Cre for recombinase-mediated cassette exchange in vitro and in adenovirus vector production. Genes Cells 16: 765–777.
20. Graham FL, Smiley J, Russell WC, Nairn R (1977) Characteristics of a human cell line transformed by DNA from human adenovirus type 5. J Gen Virol 36: 59–74.
21. Giard DJ, Aaronson SA, Todaro GJ, Arnstein P, Kersey JH, et al. (1973) In vitro cultivation of human tumors: establishment of cell lines derived from a series of solid tumors. J Natl Cancer Inst 51: 1417–1423.
22. Nakabayashi H, Taketa K, Miyano K, Yamane T, Sato J (1982) Growth of human hepatoma cells lines with differentiated functions in chemically defined medium. Cancer Res 42: 3858–3863.
23. Buchholz F, Angrand PO, Stewart AF (1998) Improved properties of FLP recombinase evolved by cycling mutagenesis. Nat Biotechnol 16: 657–662.
24. Pei Z, Kondo S, Kanegae Y, Saito I (2012) Copy number of adenoviral vector genome transduced into target cells can be measured using quantitative PCR: application to vector titration. Biochem Biophys Res Commun 417: 945–950.
25. Heishi M, Ichihara J, Teramoto R, Itakura Y, Hayashi K, et al. (2006) Global gene expression analysis in liver of obese diabetic db/db mice treated with metformin. Diabetologia 49: 1647–1655.
26. Matsui T, Takano M, Yoshida K, Ono S, Fujisaki C, et al. (2012) Neural stem cells directly differentiated from partially reprogrammed fibroblasts rapidly acquire gliogenic competency. Stem Cells 30: 1109–1119.
27. Ishida N, Hayashi K, Hoshijima M, Ogawa T, Koga S, et al. (2002) Large scale gene expression analysis of osteoclastogenesis in vitro and elucidation of NFAT2 as a key regulator. J Biol Chem 277: 41147–41156.
28. Lockhart DJ, Dong H, Byrne MC, Follettie MT, Gallo MV, et al. (1996) Expression monitoring by hybridization to high-density oligonucleotide arrays. Nat Biotechnol 14: 1675–1680.
29. Kaushal D, Naeve CW (2004) Analyzing and visualizing expression data with Spotfire. Curr Protoc Bioinformatics Chapter 7: Unit 7 9.
30. Saito I, Groves R, Giulotto E, Rolfe M, Stark GR (1989) Evolution and stability of chromosomal DNA coamplified with the CAD gene. Mol Cell Biol 9: 2445–2452.
31. Nakano M, Odaka K, Takahashi Y, Ishimura M, Saito I, et al. (2005) Production of viral vectors using recombinase-mediated cassette exchange. Nucleic Acids Res 33: e76.
32. Baba Y, Nakano M, Yamada Y, Saito I, Kanegae Y (2005) Practical range of effective dose for Cre recombinase-expressing recombinant adenovirus without cell toxicity in mammalian cells. Microbiol Immunol 49: 559–570.
33. Pei Z, Shi G, Kondo S, Ito M, Maekawa A, et al. (2013) Adenovirus vectors lacking virus-associated RNA expression enhance shRNA activity to suppress hepatitis C virus replication. Sci Rep 3: 3575.
34. Aparicio O, Razquin N, Zaratiegui M, Narvaiza I, Fortes P (2006) Adenovirus virus-associated RNA is processed to functional interfering RNAs involved in virus production. J Virol 80: 1376–1384.
35. Bennasser Y, Chable-Bessia C, Triboulet R, Gibbings D, Gwizdek C, et al. (2011) Competition for XPO5 binding between Dicer mRNA, pre-miRNA and viral RNA regulates human Dicer levels. Nat Struct Mol Biol 18: 323–327.
36. Andersson MG, Haasnoot PC, Xu N, Berenjian S, Berkhout B, et al. (2005) Suppression of RNA interference by adenovirus virus-associated RNA. J Virol 79: 9556–9565.
37. Subramanian T, Zhao LJ, Chinnadurai G (2013) Interaction of CtBP with adenovirus E1A suppresses immortalization of primary epithelial cells and enhances virus replication during productive infection. Virology 443: 313–320.
38. Boyd JM, Subramanian T, Schaeper U, La Regina M, Bayley S, et al. (1993) A region in the C-terminus of adenovirus 2/5 E1a protein is required for association with a cellular phosphoprotein and important for the negative modulation of T24-ras mediated transformation, tumorigenesis and metastasis. EMBO J 12: 469–478.
39. Chinnadurai G (2002) CtBP, an unconventional transcriptional corepressor in development and oncogenesis. Mol Cell 9: 213–224.
40. Yang J, Everett AD (2009) Hepatoma-derived growth factor represses SET and MYND domain containing 1 gene expression through interaction with C-terminal binding protein. J Mol Biol 386: 938–950.
41. Turner J, Crossley M (2001) The CtBP family: enigmatic and enzymatic transcriptional co-repressors. Bioessays 23: 683–690.
42. Nakai M, Komiya K, Murata M, Kimura T, Kanaoka M, et al. (2007) Expression of pIX gene induced by transgene promoter: possible cause of host immune response in first-generation adenoviral vectors. Hum Gene Ther 18: 925–936.

OPEN ACCESS Freely available online

PLOS | PATHOGENS

Amphipathic α-Helices in Apolipoproteins Are Crucial to the Formation of Infectious Hepatitis C Virus Particles

Takasuke Fukuhara[1☯], Masami Wada[1☯], Shota Nakamura[2], Chikako Ono[1], Mai Shiokawa[1], Satomi Yamamoto[1], Takashi Motomura[1], Toru Okamoto[1], Daisuke Okuzaki[3], Masahiro Yamamoto[4], Izumu Saito[5], Takaji Wakita[6], Kazuhiko Koike[7], Yoshiharu Matsuura[1]*

1 Department of Molecular Virology, Research Institute for Microbial Diseases, Osaka University, Osaka, Japan, **2** Department of Infection Metagenomics, Research Institute for Microbial Diseases, Osaka University, Osaka, Japan, **3** DNA-Chip Developmental Center for Infectious Diseases, Research Institute for Microbial Diseases, Osaka University, Osaka, Japan, **4** Department of Immunoparasitology, Research Institute for Microbial Diseases, Osaka University, Osaka, Japan, **5** Laboratory of Molecular Genetics, Institute of Medical Science, University of Tokyo, Tokyo, Japan, **6** Department of Virology II, National Institute of Infectious Diseases, Tokyo, Japan, **7** Department of Gastroenterology, Graduate School of Medicine, University of Tokyo, Tokyo, Japan

Abstract

Apolipoprotein B (ApoB) and ApoE have been shown to participate in the particle formation and the tissue tropism of hepatitis C virus (HCV), but their precise roles remain uncertain. Here we show that amphipathic α-helices in the apolipoproteins participate in the HCV particle formation by using zinc finger nucleases-mediated apolipoprotein B (ApoB) and/or ApoE gene knockout Huh7 cells. Although Huh7 cells deficient in either ApoB or ApoE gene exhibited slight reduction of particles formation, knockout of both ApoB and ApoE genes in Huh7 (DKO) cells severely impaired the formation of infectious HCV particles, suggesting that ApoB and ApoE have redundant roles in the formation of infectious HCV particles. cDNA microarray analyses revealed that ApoB and ApoE are dominantly expressed in Huh7 cells, in contrast to the high level expression of all of the exchangeable apolipoproteins, including ApoA1, ApoA2, ApoC1, ApoC2 and ApoC3 in human liver tissues. The exogenous expression of not only ApoE, but also other exchangeable apolipoproteins rescued the infectious particle formation of HCV in DKO cells. In addition, expression of these apolipoproteins facilitated the formation of infectious particles of genotype 1b and 3a chimeric viruses. Furthermore, expression of amphipathic α-helices in the exchangeable apolipoproteins facilitated the particle formation in DKO cells through an interaction with viral particles. These results suggest that amphipathic α-helices in the exchangeable apolipoproteins play crucial roles in the infectious particle formation of HCV and provide clues to the understanding of life cycle of HCV and the development of novel anti-HCV therapeutics targeting for viral assembly.

Citation: Fukuhara T, Wada M, Nakamura S, Ono C, Shiokawa M, et al. (2014) Amphipathic α-Helices in Apolipoproteins Are Crucial to the Formation of Infectious Hepatitis C Virus Particles. PLoS Pathog 10(12): e1004534. doi:10.1371/journal.ppat.1004534

Editor: Timothy L. Tellinghuisen, The Scripps Research Institute, United States of America

Received August 3, 2014; **Accepted** October 21, 2014; **Published** December 11, 2014

Data Availability: The authors confirm that all data underlying the findings are fully available without restriction. All relevant data are within the paper and its Supporting Information files except for the cDNA array data of GSE32886 which is available from GEO (Gene Expression Omnibus) under the accession number GSE32886.

Funding: This work was supported in part by grants-in-aid from the Japanese Ministry of Health, Labor, and Welfare (Research on Hepatitis), the Japanese Ministry of Education, Culture, Sports, Science, and Technology, the Naito Foundation, and the Takeda Science Foundation. The funders had no role in study design, data collection and analysis, decision to publish, or preparation of the manuscript.

Competing Interests: The authors have declared that no competing interests exist.

* Email: matsuura@biken.osaka-u.ac.jp

☯ *These authors contributed equally to this work.*

Introduction

More than 160 million individuals worldwide are infected with hepatitis C virus (HCV), and cirrhosis and hepatocellular carcinoma induced by HCV infection are life-threatening diseases [1]. Current standard therapy combining peg-interferon (IFN), ribavirin (RBV) and a protease inhibitor has achieved a sustained virological response (SVR) in over 80% of individuals infected with HCV genotype 1 [2]. In addition, many antiviral agents targeting non-structural proteins and host factors involved in HCV replication have been applied in clinical trials [3,4].

In vitro systems have been developed for the study of HCV infection and have revealed many details of the life cycle of HCV. By using pseudotype particles bearing HCV envelope proteins and RNA replicon systems, many host factors required for entry and RNA replication have been identified, respectively [5,6]. In addition, development of a robust *in vitro* propagation system of HCV based on the genotype 2a JFH1 strain (HCVcc) has gradually clarified the mechanism of assembly of HCV particles [7,8]. It has been shown that the interaction of NS2 protein with structural and non-structural proteins facilitates assembly of the viral capsid and formation of infectious particles at the connection site between the ER membrane and the surface of lipid droplets (LD) [9]. On the other hand, very low density lipoprotein (VLDL) associated proteins, including apolipoprotein B (ApoB), ApoE, and microsomal triglyceride transfer protein (MTTP), have been shown to play crucial roles in the formation of infectious HCV particles [10–12]. Generally, ApoA, ApoB, ApoC and ApoE bind the surface of lipoprotein through the interaction between amphipathic α-helices and ER-derived membrane [13,14]. This

Author Summary

In vitro systems have been developed for the study of hepatitis C virus (HCV) infection and have revealed many details of the life cycle of HCV. Apolipoprotein B (ApoB) and ApoE have been shown to play crucial roles in the particle formation of HCV, based on data obtained by siRNA-mediated gene knockdown and overexpression of the proteins. However, precise roles of the apolipoproteins in HCV assembly have not been elucidated yet. In this study, we show that infectious particle formation of HCV in Huh7 cells was severely impaired by the knockout of both ApoB and ApoE genes by artificial nucleases, and this reduction was cancelled by the expression of not only ApoE, but also other exchangeable apolipoproteins, including ApoA1, ApoA2, ApoC1, ApoC2 and ApoC3. In addition, expression of amphipathic α-helices in the exchangeable apolipoproteins restored the infectious particle formation in the double-knockout cells through an interaction with viral particles. These results provide clues to the understanding of life cycle of HCV and the development of novel antivirals to HCV.

binding of apolipoproteins enhances the stability and hydrophilicity of lipoprotein. However, the specific roles played by the apolipoproteins in HCV particle formation are controversial. Gastaminza et al. demonstrated that ApoB and MTTP are cellular factors essential for an efficient assembly of infectious HCV particles [10]. However, studies by other groups demonstrated that ApoE is a major determinant of the infectivity and particle formation of HCV, and the ApoE fraction is highly enriched with infectious particles [11]. In addition, Mancone et al. showed that ApoA1 is required for production of infectious particles of HCV [15]. However, the evidence of the involvement of apolipoproteins in HCV particle formation is dependent on knockdown data and exogenous expression of the apolipoproteins, and thus the precise mechanisms of participation of the apolipoproteins in HCV assembly have not been elucidated [10,11,16].

Recently, several novel genome editing techniques have been developed, including methods using zinc finger nucleases (ZFN), transcription activator like-effector nucleases (TALEN) and CRISPR/Cas9 systems [17–19]. DNA double strand breaks (DSBs) induced by these artificial nucleases can be repaired by error-prone non-homologous end joining (NHEJ), resulting in mutant mice or cell lines carrying deletions, insertions, or substitutions at the cut site. To clarify the detailed function of gene family with redundant functions, the generation of animals or cell lines carrying multiple mutated genes may be essential.

In this study, Huh7 cell lines deficient in both ApoB and ApoE genes were established by using ZFNs and revealed that ApoB and ApoE redundantly participate in the formation of infectious HCV particles. Interestingly, the expression of other exchangeable apolipoproteins, i.e., ApoA1, ApoA2, ApoC1, ApoC2 and ApoC3, facilitated HCV assembly in ApoB and ApoE double-knockout cells. In addition, the expression of amphipathic α-helices in the exchangeable apolipoproteins restored the production of infectious particles in the double-knockout cells through an interaction with viral particles.

Results

Several apolipoproteins participate in the production of infectious viral particles

First, we compared expression levels of apolipoproteins between hepatocyte and hepatic cancer cell lines including Huh7 and HepG2 cells (Fig. 1A and B). The web-based search engine NextBio (NextBio, Santa Clara, CA) revealed that ApoB, ApoH and the exchangeable apolipoproteins ApoA1, ApoA2, ApoC1, ApoC2, ApoC3, and ApoE are highly expressed in human liver tissues (Fig. 1A). On the other hand, the expressions of ApoA1, ApoC1, ApoC2, ApoC3 and ApoH in hepatic cancer cell lines were suppressed compared to those in hepatocytes (Fig. 1B). To examine the roles of apolipoproteins in the formation of infectious HCV particles, the effects of knockdown of ApoA2, ApoB and ApoE on the infectious particle production in the supernatants were determined in Huh7 cells by focus forming assay (Fig. 1C). The transfection of siRNAs targeting to ApoA2, ApoB and ApoE significantly suppressed the production of infectious HCV particles. This inhibitory effect is well consistent with the high level of expression of these apolipoproteins in the hepatic cancer cell lines, suggesting that the apolipoproteins involved in HCV assembly are dependent on the expression pattern in hepatic cancer cell lines, including Huh7 cells [20]. Therefore, we examined the effects of exogenous expression of the apolipoproteins highly expressed in the liver tissues on the infection of HCV in the stable ApoE-knockdown Huh7 cells (Fig. 1D). In contrast to the control-knockdown cells, expression of not only ApoE but also ApoA1, ApoA2, and ApoC1 rescued the infectious particle formation in the ApoE-knockdown cells (Fig. 1E), suggesting that various exchangeable apolipoproteins participate in the efficient production of infectious HCV particles.

ApoB and ApoE have a redundant role in HCV particle formation

To obtain more convincing data on the involvement of apolipoproteins in the production of infectious HCV particles, we established knockout (KO) Huh7 cells deficient in either ApoB (B-KO1 and B-KO2) or ApoE (E-KO1 and E-KO2) by using ZFN (Figure S1). Deficiencies of ApoB or ApoE expression in these cell lines were confirmed by ELISA and immunoblotting analyses (Figure S1). First, we examined the roles of ApoB and ApoE on the entry and RNA replication of HCV by using HCV pseudotype particles (HCVpp) and subgenomic replicon (SGR) of the JFH1 strain, respectively. The B-KO and E-KO cell lines exhibited no significant effect on the infectivity of HCVpp and the colony formation of SGR (Figure S2A and Figure S2B), suggesting that ApoB and ApoE are not involved in the entry and replication processes of HCV. To examine the role of ApoB and ApoE in the propagation of HCV, HCVcc was inoculated into parental, B-KO and E-KO cell lines at an MOI of 1, and intracellular viral RNA and infectious titers in the supernatants were determined (Figure S2C and Figure S2D). Although RNA replication and infectious particle formation in B-KO cells upon infection with HCV were comparable with those in parental Huh7 cells, E-KO cells exhibited slight reduction of particle formation, and the expression of ApoE in E-KO cells rescued infectious particle formation (Figure S2C, Figure S2D, Figure S2E). Next, to examine the redundant role of ApoB, the effect of knockdown of ApoB on HCV assembly was determined in parental and E-KO Huh7 cell lines (Fig. 2A). Knockdown of ApoB in E-KO cells resulted in a more efficient reduction of infectious particle production than that in parental Huh7 cells, suggesting that ApoB and ApoE have a redundant role in the formation of infectious HCV particles.

To further confirm the redundant role of ApoB and ApoE in the HCV life cycle, especially in the particle formation, 2 clones of ApoB and ApoE double-knockout (BE-KO1 and BE-KO2) Huh7 cells were established by ZFNs (Figure S3A and Figure S3B). The lack of ApoB and ApoE expressions was confirmed by immunoblotting and ELISA analyses (Figure S3C, Figure S3D, Figure

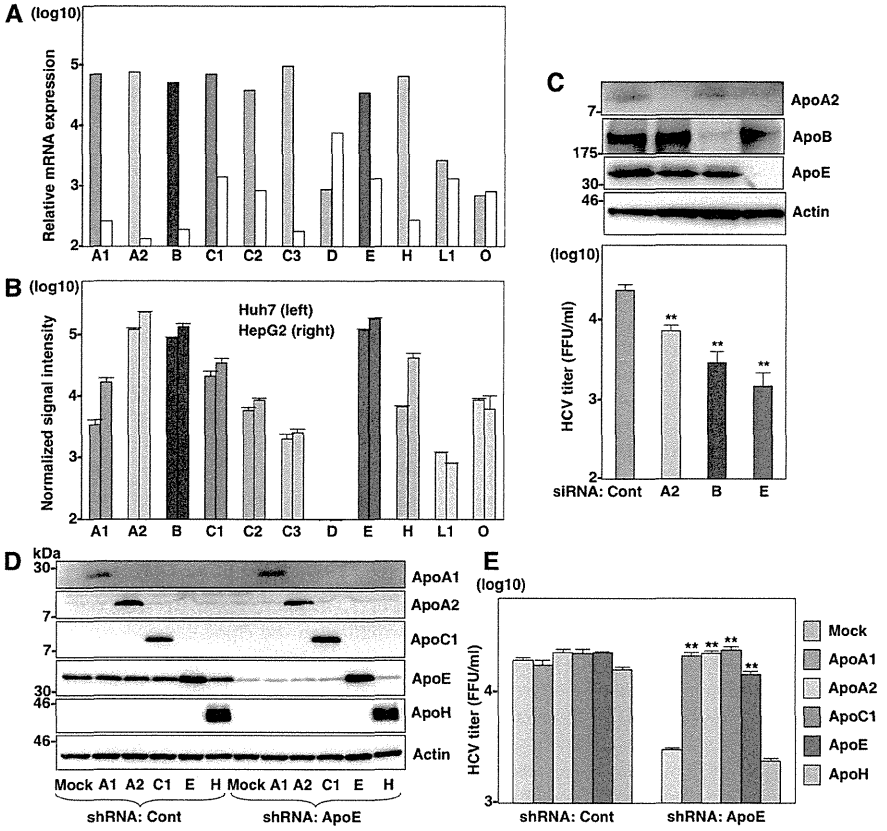

Figure 1. Several apolipoproteins participate in HCV propagation. (A) Relative mRNA expression of the apolipoproteins in the liver tissues (left columns) was determined using the NextBio Body Atlas application. The median expression (right columns) was calculated across all 128 human tissues from 1,068 arrays using the Affymetrix GeneChip Human Genome U133 Plus 2.0 Array. mRNA expression for each gene was log10 transformed. (B) Log10 transformed, normalized signal intensity of the apolipoproteins in Huh7 (left columns) and HepG2 (right columns) cells were extracted from previously published expression microarray dataset GSE32886. (C) Huh7 cells infected with HCVcc at an MOI of 1 at 6 h post-transfection with siRNAs targeting ApoA2 (A2), ApoB (B), ApoE (E) and control (Cont), and expression levels of apolipoproteins (upper panel) and infectious titers in the culture supernatants (lower panel) were determined by immunoblotting and a focus-forming assay at 72 h post-infection, respectively. (D) ApoA1, ApoA2, ApoC1, ApoE and ApoH were exogenously expressed in control and ApoE-knockdown Huh7 cells by lentiviral vectors. Expressions of the apolipoproteins were determined by immunoblotting analysis. (E) Infectious titers in the culture supernatants of control and ApoE-knockdown Huh7 cells expressing the apolipoproteins were determined by focus-forming assay at 72 h post-infection. In all cases, asterisks indicate significant differences (*, $P<0.05$; **, $P<0.01$) versus the results for control cells.
doi:10.1371/journal.ppat.1004534.g001

S3E). The BE-KO cell lines also exhibited no significant effect on the infectivity of HCVpp (Fig. 2B) and the colony formation of SGR (Fig. 2C). Next, we examined the redundant role of ApoB and ApoE on the propagation of HCVcc. Upon infection with HCVcc at an MOI of 1, infectious titers in the supernatants of BE-KO1 and BE-KO2 cells were 50 to 100 times lower than those of parental Huh7 cells at 72 h post-infection, while the level of intracellular RNA replication was comparable (Fig. 2D and E). In addition, exogenous expression of ApoE in BE-KO (ApoE-res) cells rescued the production of infectious viral particles to levels comparable to those in parental Huh7 cells (Fig. 2F and G), suggesting that ApoB and ApoE redundantly participate in the particle formation of HCV.

MTTP participates in HCV particle formation through the maturation of ApoB

It is difficult to determine the roles of ApoB in the particle formation of HCV, because ApoB is too large (550 kDa) to obtain cDNA for expression. However, previous reports have shown that expression of MTTP facilitates the secretion of ApoB [21]. To further clarify the roles of ApoB in the life cycle of HCV, we established knockout Huh7 cell lines deficient in MTTP (M-KO1 and M-KO2) and in both ApoE and MTTP (EM-KO1 and EM-KO2) by using the ZFN and CRISPR/Cas9 system (Figure S4A and Figure S4E). The lack of MTTP, ApoB and ApoE expressions was confirmed by immunoblotting and ELISA analyses (Figure Figure S4B, Figure S4C, Figure S4D, Figure S4F, Figure S4G, Figure S4H). As previously reported, the secretion of ApoB was completely abrogated in M-KO and EM-KO cells, while the mRNA levels of ApoB were comparable among Huh7, M-KO and EM-KO cells (Figure S4I). To examine the roles of MTTP in the assembly of HCV through the secretion of ApoB, HCVcc was inoculated into the Huh7, B-KO, M-KO, E-KO, BE-KO and EM-KO cell lines at an MOI of 1, and intracellular HCV genomes and infectious titers in the supernatants were determined (Fig. 3A–C). Although intracellular RNA replication in M-KO and EM-KO cells was comparable with that in Huh7, B-KO, E-KO and BE-KO cells (Fig. 3B), infectious titers in the supernatants of EM-KO cells were severely impaired as seen in BE-KO cells, while those of M-KO cells were comparable to those of parental Huh7cells (Fig. 3C), suggesting that MTTP participates

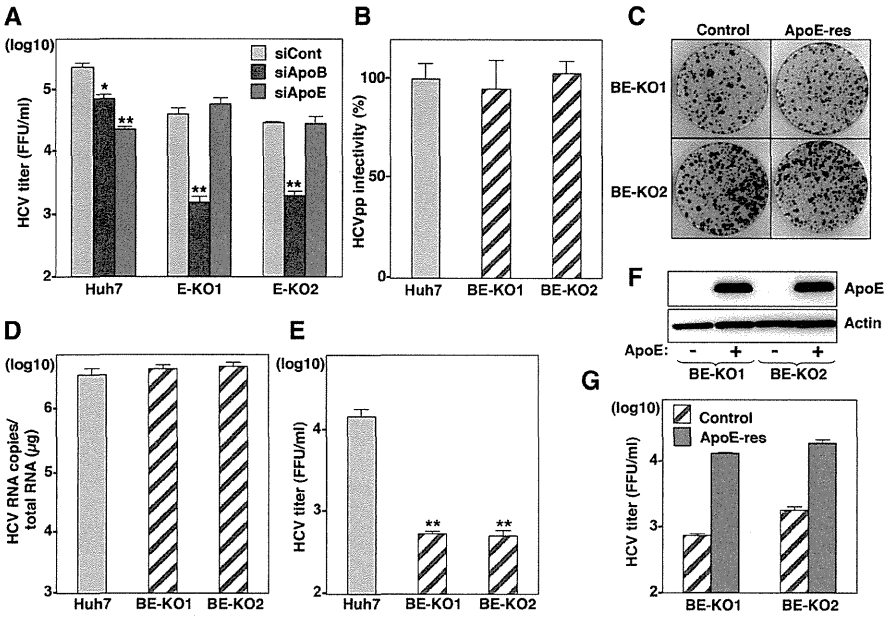

Figure 2. ApoB and ApoE redundantly participate in the formation of infectious HCV particles. (A) Huh7 and E-KO1 cells were infected with HCVcc at an MOI of 1 at 6 h post-transfection with siRNAs targeting ApoB or ApoE, and infectious titers in the culture supernatants were determined by focus-forming assay at 72 h post-infection. (B) HCVpp were inoculated into Huh7, BE-KO1 and BE-KO2 cells, and luciferase activities were determined at 48 h post-infection. (C) A subgenomic HCV RNA replicon of the JFH1 strain was electroporated into BE-KO1 and BE-KO2 cells with/without expression of ApoE by lentiviral vector (ApoE-res), and the colonies were stained with crystal violet at 31 days post-electroporation after selection with 400 μg/ml of G418. Huh7, BE-KO1 and BE-KO2 cells were infected with HCVcc at an MOI of 1, and intracellular HCV RNA (D) and infectious titers in the supernatants (E) were determined at 72 h post-infection by qRT-PCR and focus-forming assay, respectively. (F) Exogenous expression of ApoE in BE-KO1 and BE-KO2 cells by lentiviral vector was determined by immunoblotting analysis. (G) Infectious titers in the culture supernatants of BE-KO1 (gray bars) and ApoE-res cells (red bars) infected with HCVcc at an MOI of 1 were determined at 72 h post-infection by focus-forming assay.
doi:10.1371/journal.ppat.1004534.g002

in the HCV assembly through the regulation of ApoB secretion. To further confirm the roles of MTTP in HCV assembly through ApoB secretion, the effects of exogenous expression of MTTP in EM-KO cells on the infectious particle formation of HCV were determined. Immunoblotting and ELISA analyses revealed that exogenous expression of MTTP rescued the secretion of ApoB into the supernatants of EM-KO cells (Fig. 3D and E), while expression of ApoE or MTTP in both BE-KO and EM-KO cells exhibited no effect on the intracellular RNA replication (Fig. 3F). Although exogenous expression of ApoE rescued the infectious particle formation of HCV in both BE-KO and EM-KO cells, expression of MTTP rescued the particle formation in EM-KO cells but not in BE-KO cells (Fig. 3G), supporting the notion that MTTP plays a crucial role in the HCV assembly through the maturation of ApoB.

Exchangeable apolipoproteins redundantly participate in the assembly of infectious HCV particles

Next, to examine the roles played in HCV particles formation by other apolipoproteins highly expressed in the liver (Fig. 1A), the expressions of ApoA1, ApoA2, ApoC1, ApoC2, ApoC3 and ApoH in BE-KO1 cells were suppressed by siRNAs (Fig. 4A and Figure S5). While knockdown of ApoA1, ApoC3 and ApoH exhibited no effect, that of ApoA2, ApoC1 and ApoC2 significantly inhibited the release of infectious particles, which was consistent with the expression pattern of endogenous apolipoproteins except for ApoH in Huh7 cells (Fig. 1B), suggesting that not only ApoB and ApoE but also other exchangeable apolipoproteins participate in HCV particle formation. To confirm the redundant role of these apolipoproteins on the infectious particle formation, the effects of exogenous expression of these apolipoproteins on the propagation of HCVcc in BE-KO1 cells were determined. ApoA1, ApoA2, ApoC1, ApoC2, ApoC3, ApoE and ApoH were expressed by lentiviral vector in BE-KO1 cells (Fig. 4B upper panel). The expressions of ApoA1, ApoA2, ApoC1, ApoC2, ApoC3 and ApoE but not of ApoH enhanced extracellular HCV RNA, while they exhibited no effect on intracellular HCV RNA (Fig. 4C). In addition, the expressions of these exchangeable apolipoproteins enhanced the infectious particle formation in the supernatants of BE-KO1 cells (Fig. 4B lower panel). On the other hand, the expression of nonhepatic apolipoproteins, including ApoD, ApoL1, and ApoO, exhibited no effect on HCV particle formation in BE-KO1 cells (Figure S6). These results suggest that exogenous expression of not only the ApoE but also the ApoA and ApoC families can compensate for the impairment of HCV particle formation in BE-KO1 cells. Interestingly, specific infectivity (infectious titers/viral RNA levels in supernatants) was also enhanced by the expression of ApoA1, ApoA2, ApoC1, ApoC2, ApoC3 and ApoE, suggesting that these apolipoproteins participate in the infectious but not non-infectious particle formation of HCV (Fig. 4D). Previous reports have suggested that the expressions of Claudin1 (CLDN1), miR-122 and ApoE facilitate the production of infectious particles in nonhepatic 293T cells [16]. Therefore, the effects of exogenous expression of exchangeable apolipoproteins on particle formation were examined in 293T cells expressing CLDN1 and miR-122 (293T-CLDN/miR-122 cells). Exogenous expression of ApoA1, ApoA2, ApoC1, ApoC2, ApoC3 and ApoE, but not of ApoH by lentiviral vector facilitated the production of infectious

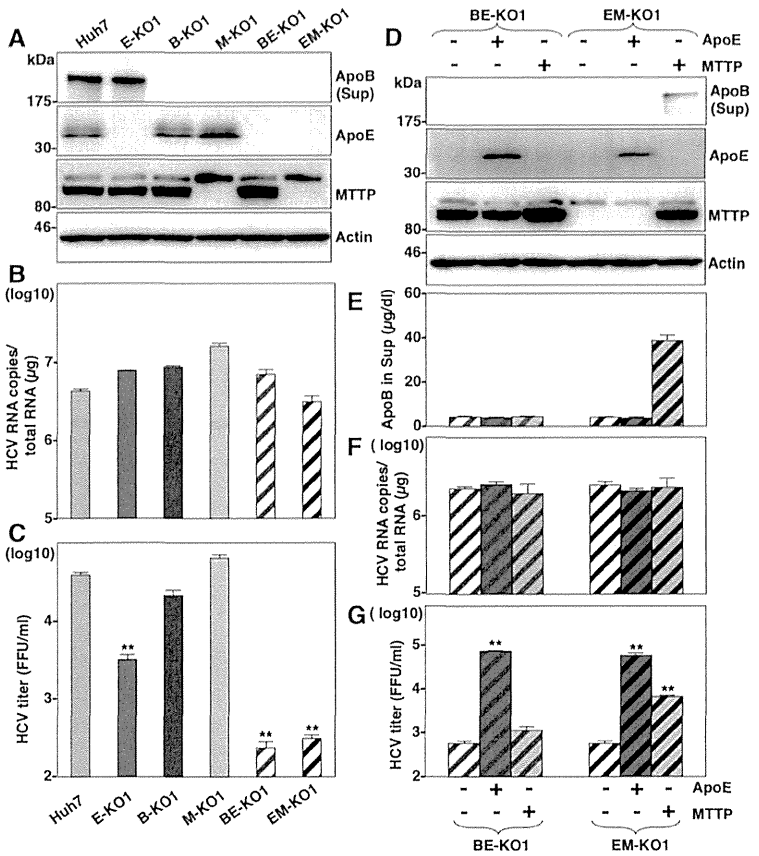

Figure 3. MTTP participates in the formation of infectious HCV particles through the maturation of ApoB. (A) Expressions of ApoB, ApoE and MTTP in Huh7, B-KO1, M-KO1, E-KO1, BE-KO1 and EM-KO1 cells were determined by immunoblotting analysis. Cells were infected with HCVcc at an MOI of 1, and intracellular HCV RNA (B) and infectious titers in the supernatants (C) were determined at 72 h post-infection by qRT-PCR and focus-forming assay, respectively. The expressions of ApoB, ApoE and MTTP in BE-KO1 and EM-KO1 cells with/without expression of ApoE or MTTP by lentiviral vector were determined by immunoblotting (D) and ELISA (E). Cells were infected with HCVcc at an MOI of 1, and intracellular HCV RNA (F) and infectious titers in the supernatants (G) were determined at 72 h post-infection by qRT-PCR and focus-forming assay, respectively.
doi:10.1371/journal.ppat.1004534.g003

HCV particles in 293T-CLDN/miR-122 cells (Fig. 4E). On the other hand, the expression of ApoE exhibited no effect on the propagation of Japanese encephalitis virus (JEV) and dengue virus (DENV) (Figure S7) in BE-KO1 cells. These results suggest that the exchangeable apolipoproteins and ApoB redundantly and specifically participate in the formation of HCV particles.

To examine the role of exchangeable apolipoproteins in the formation of other genotypes of HCV, the effect of exogenous expression of these apolipoproteins on the propagation of genotype 1b and 3a chimeric HCVcc, TH/JFH1 and S310/JFH1 viruses in BE-KO1 cells was determined (Fig. 5) [22,23]. As seen in infection with HCVcc (JFH1), expression of ApoA1, ApoA2, ApoC1, ApoC2, ApoC3 and ApoE enhanced the formation of infectious particles of TH/JFH1 and S310/JFH1 chimeric viruses. These results suggest that ApoA1, ApoA2, ApoC1, ApoC2, ApoC3 and ApoE redundantly participate in the efficient formation of infectious HCV particles of genotypes 1b, 2a and 3a.

Apolipoproteins participate in the post-envelopment step of particle formation

To determine the details of the assembly of infectious HCV particles in the BE-KO1 cells, intracellular infectious titers were determined in Huh7, BE-KO1 and ApoE-res cells by using the freeze and thaw method. Not only intracellular but also extracellular infection titers were impaired in BE-KO1 cells compared with those in parental and ApoE-res cells (Fig. 6A), suggesting that intracellular particle formation is impaired by deficiencies in the expression of ApoB and ApoE. Previous reports have shown that the recruitment of viral proteins around LD and redistribution of LD are essential for HCV assembly [24]. To clarify the roles of the exchangeable apolipoproteins on HCV assembly in more detail, we examined the intracellular localization of viral proteins, LD and ER in BE-KO1 and ApoE-res cells. The localization of core proteins around LD and the membranous-web structure forming the replication complex were observed in BE-KO1 cells upon infection with HCVcc, as reported in parental Huh7 cells (Fig. 6B, 6C and Figure S8). However, greater accumulation of core proteins and LD around the perinuclear region was detected in BE-KO1 cells in comparison with ApoE-res cells (Fig. 6C and 6D), supporting the notion that apolipoproteins participate in the infectious particle formation in HCV rather than viral RNA replication. Previous studies revealed that core proteins were mainly localized on the ER membrane upon infection with the genotype 2a Jc1 strain-based HCVcc (HCVcc/Jc1), and inhibition of capsid assembly and envelopment caused accumulation of core proteins on the surface of LD [25–27]. In ApoE-res cells, core proteins of HCVcc/Jc1 were mainly localized on the